

UNIVERSITY OF CALGARY

Refined Models of Extensible Elastic Beams for Studying Nonlinear Vibrations

by

Mehdi Tabe Arjmand

A THESIS

SUBMITTED TO THE FACULTY OF GRADUATE STUDIES
IN PARTIAL FULFILLMENT OF THE REQUIREMENTS FOR THE
DEGREE OF MASTER OF SCIENCE

DEPARTMENT OF MECHANICAL AND MANUFACTURING ENGINEERING

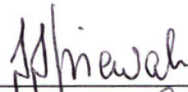
CALGARY, ALBERTA

January, 2011

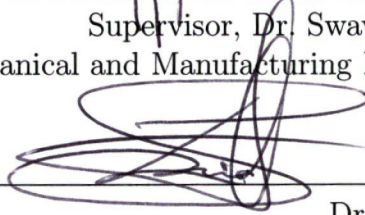
© Mehdi Tabe Arjmand 2011

UNIVERSITY OF CALGARY
FACULTY OF GRADUATE STUDIES

The undersigned certify that they have read, and recommend to the Faculty of Graduate Studies for acceptance, a thesis entitled "Refined Models of Extensible Elastic Beams for Studying Nonlinear Vibrations" submitted by Mehdi Tabe Arjmand in partial fulfillment of the requirements for the degree of Master of Science.



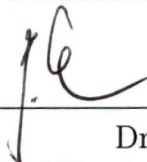
Supervisor, Dr. Swavik Spiewak
Department of Mechanical and Manufacturing Engineering



Dr. Les Sudak
Department of Mechanical and Manufacturing Engineering



Dr. Qiao Sun
Department of Mechanical and Manufacturing Engineering



Dr. Joern Davidsen
Department of Physics and Astronomy

January 25, 2011

Date

Abstract

This research is aimed at analyzing the equations governing large amplitude in-plane forced vibrations of an extensible Euler-Bernoulli beam under transversal excitation. The axial displacement of the beam is taken into account as well as the transversal motion, rotary inertia terms and damping forces.

Employing Galerkin mode shape expansion method and expanding the non-linear terms into Taylor series, the non-linear partial differential equations (PDEs) of motion are approximated by a set of coupled ordinary differential equations (ODEs). The effect of higher order terms in Taylor series expansion and also effect of including higher order mode shapes in Galerkins method are studied. The static behavior, free (non-linear) vibrations and forced vibrations of an elastic extensible beam are studied and the results are compared with those obtained from previous simplified derivations published by other researchers.

Employing the Lyapunov exponent measure, we find the relationship between excitation parameters and chaotic vibrations of the beam. We find that the simplified models exhibit significantly different chaotic behavior in comparison with the more accurate model proposed in this thesis.

Table of Contents

Abstract	ii
Table of Contents	iii
List of Figures	v
1 Introduction and Literature Review	4
1.1 Applications	4
1.2 Mathematical Models	5
1.2.1 Beam Theories	6
1.2.2 Beam Equations	7
1.3 Solving The Beam Equations	9
1.3.1 Nonlinear Systems and Chaos	10
1.3.2 Literature Review	11
1.4 Contributions	12
1.5 Organization	13
2 Formulation of The Problem	15
2.1 Problem Statement	15
2.2 Calculus of Variations	16
2.2.1 General Functionals	18
2.3 Preliminaries	19
2.3.1 Coordinate Systems	19
2.3.2 Basic Relationships	20
2.3.3 Beam Curvature	22
2.3.4 Constitutive Equations	23
2.4 Deriving the Equation of Beam Motion Using Lagrangian mechanics	24
2.4.1 Kinetic Energy	24
2.4.2 Potential Energy	25
2.4.3 Work of Nonconservative Forces	25
2.5 Equations of Motion	26
2.6 Derivations Based on the Newtonian Framework	26
2.7 Previous Derivations	32
3 Static Solution	38
3.1 Static Equations	38
3.1.1 The Buckling Load	41
3.2 Equilibrium Paths	42
4 Dynamic Solution	49
4.1 Linearized Equations	49
4.2 Nonlinear Equations	52
4.2.1 Galerkin Method	52
4.2.2 Case I: First Mode Shape Expansion	55
4.2.3 Case II: First & Second Mode Shape Expansion	58
4.3 The Effect of Including Higher Order Mode Shapes	65

5	Free Vibrations	70
5.1	Free Vibrations of Extensible Beams	70
6	Forced Vibrations and Chaos	79
6.1	Lyapunov Exponents	79
7	Conclusions and Future Work	88
A	Runge-Kutta 7^{th} and 8^{th} order	91
	Bibliography	95

List of Figures

1.1	A schematic representation of an axially loaded buckled beam	6
2.1	A schematic representation of the beam under study	16
2.2	An element of the beam before and after deformation	20
2.3	Infinitesimal element of the beam	21
2.4	Free body diagram for an element of the beam	27
2.5	Alternative free body diagram for the beam element	29
3.1	Buckling load of a 2D extensible beam	43
3.2	Equilibrium path for a buckled beam, $\mu = 10$, $\lambda = 1.01\lambda_{cr}$	46
3.3	Difference between the exact solution of 2D extensible beam and (a) 1D Extensible and (b) Inextensible beam	47
3.4	Load-paths for 2D extensible, 1D extensible and inextensible beam, $\mu = 150$	48
4.1	The error in calculation of maximum deflection (between Taylor series approximation and exact non-linear terms), $\lambda = 1.5\lambda_{cr}$	53
4.2	The error in calculation of maximum deflection (between Taylor series approximation and exact non-linear terms), $\mu = 10$	54
4.3	Dynamics of maximum transversal deflection of the beam in Case I and Case II, $\mu = 10$, $\lambda = 0$	66
4.4	Dynamics of maximum transversal deflection of the beam in Case I and Case II, $\mu = 100$, $\lambda = 0$	67
4.5	Frequency difference between Case I and Case II, $\lambda = 0$	67
4.6	Dynamics of maximum transversal deflection of the beam in Case I and Case II, $\mu = 10$, $\lambda = 5$	68
4.7	Dynamics of maximum transversal deflection of the beam in Case I and Case II, $\mu = 10$, $\lambda = 9$	69
5.1	Axial and transversal displacements versus time	71
5.2	Transversal vibration for $\mu = 10$ and different values of λ	72
5.3	Influence of axial force, λ , on the natural frequency of transversal vibrations	73
5.4	Influence of the axial force, λ , on the natural frequency of transversal vibrations in different beam models, $\mu = 1000$	74
5.5	The rotary inertia effect on the natural frequency of transversal vibration, $\mu = 10$	75
5.6	Frequency response for a nonlinear system showing (a) the backbone curve for the free undamped vibrations and (b) the resonance curve for forced damped system with hardening and softening nonlinearity .	76
5.7	Amplitude versus natural frequency for different slenderness ratios, $\lambda = 0$	77

6.1	Dynamics of largest Lyapunov exponent for a beam with regular behavior	80
6.2	Dynamics of largest Lyapunov exponent for a beam with chaotic behavior	81
6.3	Largest Lyapunov exponent versus frequency of excitation for a 2D extensible beam	82
6.4	Largest Lyapunov exponent versus amplitude of excitation for a 2D extensible beam	83
6.5	Largest Lyapunov exponent versus frequency of excitation for a 1D extensible and inextensible model	84
6.6	Time history of transverse displacement for different beam models, $\mu = 10$	85
6.7	<i>Poincaré</i> map of 1D extensible and inextensible models	86
6.8	Time history of transverse displacement for different beam models, $\mu = 400$	87

Nomenclature

A	Cross-sectional area of the beam
A	Amplitude of excitation
\mathcal{A}	Nondimension amplitude of excitation
α	Parameter defined by Eq. (4.2)
c_d	Damping coefficient per unit length of the beam
C	Nondimension c_d
Δ	Total elongation of the beam
E	Modulus of elasticity
e	Elongation
e	Parameter defined by Eq. (3.28)
ϵ	Strain
$\bar{\epsilon}$	Average strain
H	X component of internal forces
\mathcal{H}	Nondimension H
I	Area moment of inertia of the beam
J	Mass moment of inertia of the beam
\mathcal{J}	Axial force due to elongation of the beam
k_1	Mass' radius of gyration
γ	Nondimension k_1

κ	Curvature
L	Length of the beam
λ	Nondimension external axial force
M	Bending moment
\mathcal{M}	Nondimension M
μ	Slenderness ratio
P	Internal normal force
P_0	External axial force
P_{cr}	Extensible beam buckling load
P_E	Euler Buckling load
Q	Shear force
ρ	Mass density per length of the beam
q_1	Axial displacement of the beam
q_2	Transversal displacement of the beam
θ	Slope of a curve
s	Length of a curve
σ	Normal stress
T	Kinetic energy
t	Time
τ	Nondimension t
u	Nondimension q_1
V	Y component of internal forces

V	Potential energy
\mathcal{V}	Nondimension V
V_a	Potential energy due to axial stress
V_b	Potential energy due to bending
v	Nondimension q_2
W_c	Work done by conservative forces
W_{nc}	Work done by nonconservative forces
w	Displacement of the base of the beam
ω	Frequency of excitation
Ω	Nondimension ω
(X, Y)	Axes in Lagrangian coordinates
(X^*, Y^*)	Axes in Eulerian coordinates
(x, y)	Undeformed position of a point of the beam
(x^*, y^*)	Deformed position of a point of the beam
ξ	Nondimension x

Chapter 1

Introduction and Literature Review

1.1 Applications

Buckled beam structures under dynamic loading are frequently encountered in various engineering applications. The beams are designed either to prevent buckling, e.g. civil structures such as bridges or buildings, or to buckle for their functionality, e.g. MEMS [32], suspension systems [38], optical measuring systems [44].

Buckled beams are bistable structures, with a two-well potential. Their nonlinear properties are exploited in actuator design, e.g. MEMS micropumps, switches, memory cells to produce relatively high displacements and forces with low actuation energies [18, 29]. Another advantage of such structures is that they can apply contact forces without the need for continued actuation power [31].

Recently a lot of attention has been drawn to applications of buckled beams in energy harvesting devices, e.g. in [31, 36, 18, 20, 3, 17]. Energy harvesting has emerged as an important new topic with the goal of fabricating devices that can generate electrical power by exploiting ambient vibrational energy. Bistability, together with its nonlinear properties, make the buckled beams ideal structures to extract energy from ambient vibrations [20, 33, 23].

One aspect of the design process of buckled beams for the aforementioned applications is the dynamic response of these structures under a variety of excitations. A significant amount of insight can be gained by investigating the mathematical model of a buckled beam. The more accurate the mathematical model is, the closer we are

to the actual problem.

1.2 Mathematical Models

A simple model that can be used to derive the governing equations of an axially loaded (buckled) beam is depicted in Fig. (1.1). The beam has mass density per length of the beam ρ , length L , cross-sectional area A , area moment of inertia I , mass moment of inertia J and modulus of elasticity E . It is statically loaded by an axial force P_0 . In the literature the buckled beam with different boundary conditions such as clamped-clamped or pinned-pinned with movable or immovable (axially restrained) ends has been studied.

In this research one end of the beam is assumed to be fixed and axially restrained, the other end, at which the external axial force is applied, can freely move in the horizontal direction. The beam has 2D motion, axial and transverse. The axial displacement is denoted by q_1 and the transverse displacement by q_2 . Both q_1 and q_2 are functions of the spatial coordinate x and time t , i.e. $q_1 \equiv q_1(x, t)$ and $q_2 \equiv q_2(x, t)$. Thus q_1 and q_2 are suitable generalized coordinates for describing the motion of this beam. Note that in general, if the plane cross-sections of the beam does not remain plane and perpendicular to the neutral axis during the vibration more generalized coordinates are needed to describe the motion of the beam.

The beam may experience transverse excitation, by means of the base excitation. A distributed damping force can also be included in the beam model. All physical properties are constant along the beam span. The material is isotropic and homogeneous.

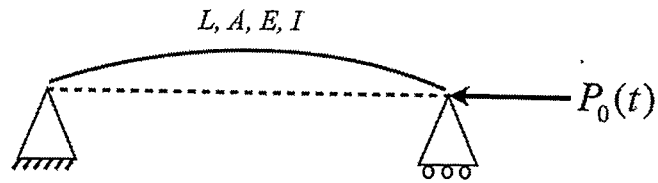


Figure 1.1: A schematic representation of an axially loaded buckled beam

1.2.1 Beam Theories

There exist four main beam theories for the investigation of beam vibrations. The four theories are the Euler-Bernoulli, Rayleigh, Shear and Timoshenko [11]. Here, a brief history of the development of the Euler-Bernoulli theory, which is most frequently used in the literature for deriving the equations of beam vibrations, is presented. In this thesis the Euler-Bernoulli theory is employed as well.

Euler-Bernoulli Theory

It was recognized by the early researchers that the bending effect is the single most important factor in the transverse vibration of a beam. The Euler-Bernoulli theory includes the strain energy due to the bending and the kinetic energy due to the transverse displacement. The Euler-Bernoulli theory dates back to the 18th century. Jacob Bernoulli (1654-1705) first discovered that the curvature of an elastic beam at any point is proportional to the bending moment at that point. Later, Jacob Bernoulli's theory was accepted by Leonhard Euler (1707-1783) in his investigation of the shape of elastic beams under various loading conditions. Many advances on the elastic curves were made by Euler. The Euler-Bernoulli beam theory, sometimes called the classical beam theory is the most commonly used because it is simple and provides

reasonable engineering approximations for many problems [11].

1.2.2 Beam Equations

Researchers have used different approaches and assumptions to model beams. In particular vibrations of beams were studied with various degrees of generality. Some of the important assumptions that have been made in deriving the equations are as follows

- (1) The amplitude of vibrations is small
- (2) Axial displacement of the beam is neglected
- (3) Extensibility of the beam is neglected
- (4) Rotary inertia is neglected

As a result, several models exist in the literature for describing the motion of buckled beams. The simplest equation, for the undamped free vibration of a beam, which can be derived based on Euler-Bernoulli theory is

$$\rho q_{2,tt} + EI q_{2,xxxx} + P_0 q_{2,xx} = 0 \quad (1.1)$$

In the above equations $q_{2,tt} \equiv \frac{\partial^2 q_2}{\partial t^2}$, $q_{2,xx} \equiv \frac{\partial^2 q_2}{\partial x^2}$ and $q_{2,xxxx} \equiv \frac{\partial^4 q_2}{\partial x^4}$. Detailed derivations for the above equation can be found in text books by Meirovitch [22], Rao [34] and Virgin [42]. In this model it is assumed that no axial displacement of the elements of the beam take place, i.e. $q_1 = 0$. This case typically exists when both ends of the beams have either the "fixed" or "pinned" constraints and their relative distance in the axial direction remains constant regardless of the transverse shape, i.e. the beam is axially restrained. In this derivation no internal axial force is considered.

A more accurate model can be derived based on the above equation by taking into account the internal axial force. This force is generated due to the extension or

stretching of the beam midplane. Eq. (1.1) is rewritten as

$$\rho q_{2,tt} + EI q_{2,xxxx} + \left(P_0 - \frac{EA}{2L} \int_0^L q_{2,x}^2 dx \right) q_{2,xx} = 0 \quad (1.2)$$

The result is an integro-partial differential equation for the transverse direction, q_2 . Henceforth this equation is referred to the *1D Extensible model*. Detailed derivations for the above equation are shown in Chapter 2. This equation was probably first proposed by Woinowsky-Krieger (1950) for the vibration of buckled beams [45]. In deriving this equation assumptions (1), (2) and (4) shown on the preceding are applied.

Another important derivation is the equation describing vibration of an inextensible elastic beam. Alturi (1973) was the first to derive and study the equation for vibration of inextensible beams [2]. The inextensibility assumption is valid when at least one end of the beam has the "free" or "guided" constraint. In this model, although a two dimensional motion of the beam is considered, but because the beam is assumed to be inextensible the axial and transverse displacements are related to each other and hence only one generalized coordinate is needed to describe to motion of the system. The equation for vibration of inextensible elastic beam has been refined by Noijen et al. (2007) in [28], including higher order terms. The result is

$$\begin{aligned} \rho q_{2,tt} + EI q_{2,xx} \left(q_{2,xx}^2 \left(1 + \frac{3}{2} q_{2,x}^2 \right) + 4 q_{2,x} q_{2,xxx} \right. \\ \left. \left(1 + \frac{1}{2} q_{2,x}^2 \right) \right) + EI q_{2,xxxx} \left(1 + q_{2,x}^2 + \frac{1}{4} q_{2,x}^4 \right) + P_0 q_{2,xx} = 0 \end{aligned} \quad (1.3)$$

A detailed derivation of the above equation is shown in Chapter 2. In deriving this equation assumptions (3) and (4) are applied. Henceforth this equation is referred to as the *Inextensible model*.

As can be seen from both 1D extensible and inextensible models, the equations are in terms of only one generalized coordinate, q_2 . By taking into account the exten-

sibility and axial displacement together, another model, referred in this thesis as *2D extensible model* is derived. The equations for 2D extensible beam are two coupled partial differential equations in terms of q_1 and q_2 . It is also possible to include the rotary inertia terms in these equations as well. A detailed derivation of 2D extensible model is shown in Chapter 2. Atanackovic (1994) has derived the equations governing free vibration of 2D extensible beam [5].

The intention in this work is to analyze the large amplitude forced vibrations, especially chaotic vibrations of an extensible elastic beam, including the axial displacement as well as rotary inertia terms, i.e. releasing assumptions (1), (2), (3) and (4).

1.3 Solving The Beam Equations

As discussed in the previous section, the dynamics of buckled beams, for 1D extensible, inextensible and 2D extensible models, is governed by nonlinear partial differential equations in space and time. The closed form solutions for these equations are unknown and, consequently, one seeks approximate solutions of the original problem.

Two common approaches to obtain approximate solutions of partial differential equations involve (1) numerical methods, and (2) analytical methods. In the numerical methods (e.g. finite differences, finite elements) one replaces the original equations by a set of nonlinear algebraic equations, which can be solved by using a variety of techniques. In the analytical methods direct techniques, such as the perturbation or discretization techniques are used. In the discretization technique a solution of the partial differential equations of a buckled beam is assumed to be the product of two functions. One is a function of time only, and the other one is a function of space.

The discretization techniques involve different methods such as the weighted residuals (e.g. Galerkin, collocation, least squares) or variational methods (e.g. Rayleigh-Ritz) [7].

In the beam studies, the Galerkin discretization method is widely used and usually the mode shapes of the beam are used as the known functions of space. This method is also called "Galerkin mode shape expansion method". In this research the Galerkin discretization method is discussed in detail in Chapter 4 and used for approximating the partial differential equations of the investigated system. The result is a set of nonlinear coupled ordinary differential equations.

1.3.1 Nonlinear Systems and Chaos

One of the main differences between linear and nonlinear systems is the existence of chaotic behavior in the latter. Chaos in dynamical system is associated with the class of motions whose responses feature a sensitive dependence upon the initial conditions. It has been proven that chaos can exist in deterministic system, i.e. systems with no random or unpredictable inputs or parameters. In chaotic systems long term prediction becomes impossible, since small differences in initial conditions can produce great differences in the final output. The existence of chaotic or unpredictable motions in classical mechanics was first pointed out by *Poincaré* [26].

There are different techniques of identifying chaos in dynamical systems such as the Fourier spectrum, *Poincaré* maps, Lyapunov exponents, Melnikov function and fractal dimensions. The *Poincaré* map is a qualitative method and the Lyapunov exponent is a quantitative measure of identifying chaos. Both methods have been employed in this work to study chaos.

1.3.2 Literature Review

During the past few decades significant research has been performed on the nonlinear vibrations of buckled beams. The 1D extensible beam model, Eq. (1.2), has been extensively used in the literature to study the vibration of elastic beams since 1950. The free vibration of 1D extensible beam has been studied by a couple of researchers, such as Burgreen (1951) and McDonald (1955) [4, 19]. The forced vibration of this model has been studied in [6, 41, 24].

In the past three decades, the effort of researchers has shifted to nonlinear dynamics of buckled beams. Holmes (1979) investigated the stability of the motion of a buckled beam and its phase space portraits using the 1D extensible model [12]. Moon (1980) and Holmes and Moon (1983) investigated chaotic motions of buckled beams under external harmonic excitations. They used a single-mode approximation to predict the onset of these chaotic motions [25, 13]. The effect of higher modes on the chaotic motion of a buckled beam was studied in [39]. Reynolds and Dowell (1996) studied the chaotic motion of a buckled beam under a harmonic excitation using a multi-mode Galerkin discretization. They used Melnikov theory in their analysis [35].

Lestari and Hanagud (2001) presented exact solutions to the nonlinear free vibrations of 1D extensible buckled beams using elliptic functions [15]. Emam and Nayfeh (2004) investigated nonlinear dynamics of a buckled beam under excitation. They found that using a single-mode approximation leads to quantitative and qualitative errors in the static and dynamic conditions [8]. Nayfeh and Emam (2008) have recently found an exact solution for the post-buckling configurations of 1D extensible buckled beams [27].

A few other works have dealt with modeling the dynamic behavior of beams with-

out considering extensibility, as in the inextensible model, Eq. (1.3). As mentioned earlier Alturi (1973) was the first to derive the equations governing the vibrations of an inextensible beam. He recognized that the first mode of inextensible beams exhibits a softening nonlinearity in contrast with that of 1D extensible beams that are of the hardening type and concluded that axial inertia is the dominant nonlinearity in inextensible beams. Mei et al. (1985) found a similar non-linearity of softening type in their investigation by employing FEM [21]. Lacarbonara and Yabuno (2006) experimentally studied the free vibrations of the inextensible model and compare the results with 1D extensible model [14]. Noijen et al. (2007) studied the chaotic vibrations of inextensible beam considering higher order modes in Galerkin method [28].

The free vibrations of undamped 2D extensible beam have been studied in [5] using the single mode Galerkin method. The exact solution for the post-buckling configurations of 2D extensible buckled beams was proposed in [16].

1.4 Contributions

The goal of this research is to find an accurate model for studying nonlinear vibrations and chaos in a buckled beam. It has been shown in this thesis that earlier works are not general enough for this purpose. In this thesis the equations governing the large amplitude in-plane forced vibrations of a damped 2D extensible beam under transverse excitation are derived. Employing the Galerkin mode shape expansion method and expanding the non-linear terms into Taylor series, the non-linear partial differential equations (PDEs) of motion are approximated by a set of ordinary differential equations (ODEs). The effect of higher order terms in Taylor series expansion and also effect of including higher order mode shapes in Galerkin's method

are studied. The free nonlinear vibrations of 2D extensible beam is studied and the results are compared with those obtained from 1D extensible and inextensible models. Employing numerical calculation of largest Lyapunov exponent and *Poincaré* map, the possibility of chaotic responses of forced vibrations of 2D extensible elastic beams is investigated. The results for chaotic vibration are compared with those obtained from 1D extensible and inextensible models.

1.5 Organization

In Chapter 2, I derive the equations governing the large amplitude forced vibrations of a damped extensible Euler-Bernoulli beam under transverse excitation. The axial displacement of the beam is taken into account as well as the transverse motion and rotary inertia terms. First, relevant aspects of calculus of variations are reviewed. The different types of coordinate systems and basic equations of the beam problem are also reviewed. By employing the Lagrangian mechanics, the equations describing the motion of an elastic beam are derived. An alternative approach based on the Newtonian framework is investigated and the general system of equations associated with boundary conditions is derived. Previous derivations, based on different assumptions are discussed. The derived equations are expressed in a nondimensionalized form.

In Chapter 3, the equation of the 2D elastic extensible beam for the static case is derived. The buckling load and the equilibrium paths when the beam buckles are investigated. The results are compared with the static behavior of the 1D extensible and inextensible models.

Chapter 4 is concerned with beam dynamics. First the linearized equations of 2D extensible elastic beam are studied. Based on the linearized equations the expressions

for natural frequencies and mode shape of the beam are derived. Employing the Galerkin mode shape expansion method and expanding the non-linear terms into a Taylor series, the non-linear partial differential equations (PDEs) of motion are approximated by a set of ordinary differential equations (ODEs). The effect of higher order terms in Taylor series expansion and also effect of including higher order mode shapes in Galerkin's method are studied. The Galerkin method is also employed to approximate the PDEs of 1D extensible and inextensible beam models.

In Chapter 5, the free nonlinear vibrations of an extensible elastic beam are studied. The effect of external axial load, the slenderness ratio and the rotary inertia on the natural frequency of the beam is investigated. Also the configuration of resonance curve is studied for different system parameters. The results are compared with those obtained from 1D extensible and inextensible models.

In Chapter 6, by numerical calculation of largest Lyapunov exponent, the possibility of chaotic responses of forced vibrations of 2D extensible elastic beams is investigated. The chaotic behavior is investigated for different amplitudes and frequencies of excitation. The results are compared with those obtained from 1D extensible and inextensible models.

In Chapter 7 conclusions and suggestions for future works are presented.

Chapter 2

Formulation of The Problem

In this chapter the derivations of equations governing the large amplitude forced vibrations of a damped extensible Euler-Bernoulli beam under transverse excitation is studied. The axial displacement of the beam is taken into account as well as the transverse motion and rotary inertia terms. First, relevant aspects of calculus of variations are reviewed. The different types of coordinate systems and basic equations of the beam problem are also reviewed. By employing the Lagrangian framework, the equations describing the motion of an elastic beam are derived. An alternative approach based on the Newtonian framework is investigated and the general system of equations associated with boundary conditions is derived. Previous derivations, based on different assumptions are discussed. The derived equations are expressed in a nondimensionalized form.

2.1 Problem Statement

I consider a straight simply supported beam of length L , cross-sectional area A , area moment of inertia I , mass moment of inertia J and modulus of elasticity E . It is statically loaded by an axial force P_0 , as shown in Fig. (2.1). One end of the beam is fixed and axially restrained, the other end at which the external axial force is applied can freely move in horizontal direction. In studying the vibrations of buckled beams, the axial force P_0 is chosen to exceed the lowest buckling load, P_{cr} , of the beam. The beam is modeled according to the Euler-Bernoulli's hypothesis, i.e.

plane cross-sections of the beam, remain plane and perpendicular to the neutral axis before and after deformation. It is also assumed that the plane cross-sections do not change their shape and area. The beam has 2D motion, axial and transverse. The axial displacement is denoted by q_1 and the transverse displacement by q_2 . Both q_1 and q_2 are functions of the spatial coordinate x and time t , i.e. $q_1 \equiv q_1(x, t)$ and $q_2 \equiv q_2(x, t)$. The beam may experience transverse excitation, by means of base excitation. Furthermore, a damping distributed force may be acting on the beam. All physical properties are constant along the beams span. The material is isotropic and homogeneous.

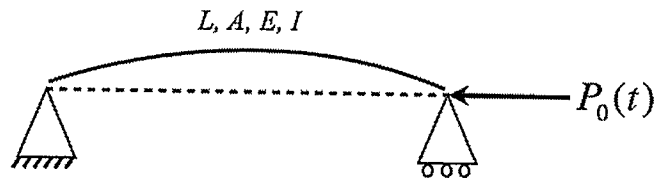


Figure 2.1: A schematic representation of the beam under study

Equations governing the extensible beam motion are derived in Lagrangian and Newtonian framework. In the following an introduction to calculus of variations, which is the foundation of Lagrangian framework, is presented.

2.2 Calculus of Variations

Calculus of variations (CV) is concerned primarily with extremizing functionals, as opposed to ordinary calculus which deals with functions. Functionals are generally functions of other functions. They are often formed as definite integrals involving unknown functions and their derivatives. The interest is in extremal functions that make

the functional attain a maximum or minimum value. An example simple functional in terms of one independent variable t , and a function $q(t)$ is

$$I(q) = \int_{t_1}^{t_2} F(t, q, q_t, q_{tt}) dt \quad (2.1)$$

where $q \equiv q(t)$, $q_t \equiv \frac{dq}{dt}$ and $q_{tt} \equiv \frac{d^2q}{dt^2}$. Functionals involving higher-order derivatives and several independent variables can also be dealt with. The objective of CV is to choose a function $\hat{q}(t)$, called an extremal, so as to minimize or maximize (extremize) the functional. Note that here it is assumed that the variations of q in the endpoints are zero. In other words, CV is concerned with finding functions that extremize integrals whose integrands contain these functions.

The application of CV is often associated with solving problems of continuum mechanics. The functionals whose extreme values are sought involve some form of the system energy. For example, many of the phenomena governing the elastic distortion of bodies can be described by employing the principle of minimum potential energy [9].

By using CV it can be shown that the necessary condition for $q(t)$ to extremize $I(q)$ shown in Eq. (2.1) is [9]

$$\frac{\partial F(\cdot)}{\partial q} - \frac{d}{dt} \left[\frac{\partial F(\cdot)}{\partial q_t} \right] + \frac{d^2}{dt^2} \left[\frac{\partial F(\cdot)}{\partial q_{tt}} \right] = 0 \quad (2.2)$$

Equation (2.2) is known as the Euler-Lagrange equation and is the differential equation that $\hat{q}(t)$ must satisfy.

In the case of time dependent distributed parameter systems there are two or more independent variables. The functionals reflect this are shown in the following example involving the time t and a spatial coordinate x as independent variables.

2.2.1 General Functionals

The Euler-Lagrange equations for functionals characterizing the investigated beams can be derived by proceeding in a similar manner as for the functional in the above example (Eq. (2.1)). The involved function, $F(\cdot)$, depends upon two independent variables and their derivatives up to and including the second order. For such a case, the functional has the form

$$I(q) = \int \int_{\Omega} F(t, x, q, q_t, q_x, q_{tx}, q_{tt}, q_{xx}) dx dt \quad (2.3)$$

where Ω is the domain in which the function $F(\cdot)$ is extremized and $q \equiv q(x, t)$, $q_x \equiv \frac{\partial q}{\partial x}$, $q_{xx} \equiv \frac{\partial^2 q}{\partial x^2}$ and $q_{tx} \equiv \frac{\partial^2 q}{\partial t \partial x}$.

The obtained Euler-Lagrange equation is [9]

$$\frac{\partial F(\cdot)}{\partial q} - \frac{\partial}{\partial t} \left[\frac{\partial F(\cdot)}{\partial q_t} \right] - \frac{\partial}{\partial x} \left[\frac{\partial F(\cdot)}{\partial q_x} \right] + \frac{\partial^2}{\partial t^2} \left[\frac{\partial F(\cdot)}{\partial q_{tt}} \right] + \frac{\partial^2}{\partial t \partial x} \left[\frac{\partial F(\cdot)}{\partial q_{tx}} \right] + \frac{\partial^2}{\partial x^2} \left[\frac{\partial F(\cdot)}{\partial q_{xx}} \right] = 0 \quad (2.4)$$

The above equation can also be extended for the case that $I \equiv I(q_1, q_2)$. In this case we will have two sets of equations. The functional is in the form of:

$$I(q_1, q_2) = \int \int_{\Omega} F(\cdot) dx dt \quad (2.5)$$

where $F(\cdot) \equiv F(t, x, q_1, q_2, q_{1,t}, q_{2,t}, q_{1,x}, q_{2,x}, q_{1,tx}, q_{2,tx}, q_{1,tt}, q_{2,tt}, q_{1,xx}, q_{2,xx})$. The corresponding Euler-Lagrange sets of equations are [9]

$$\frac{\partial F(\cdot)}{\partial q_i} - \frac{\partial}{\partial t} \left[\frac{\partial F(\cdot)}{\partial q_{i,t}} \right] - \frac{\partial}{\partial x} \left[\frac{\partial F(\cdot)}{\partial q_{i,x}} \right] + \frac{\partial^2}{\partial t^2} \left[\frac{\partial F(\cdot)}{\partial q_{i,tt}} \right] + \frac{\partial^2}{\partial t \partial x} \left[\frac{\partial F(\cdot)}{\partial q_{i,tx}} \right] + \frac{\partial^2}{\partial x^2} \left[\frac{\partial F(\cdot)}{\partial q_{i,xx}} \right] = 0, \quad i = 1, 2 \quad (2.6)$$

which indirectly define the sought functions $q_1(x, t)$ and $q_2(x, t)$. The function $F(\cdot)$ involved in this research is derived in the following.

2.3 Preliminaries

2.3.1 Coordinate Systems

In continuum mechanics one usually has a choice between two sets of coordinate systems to describe the position of material points: one set for the undeformed body (Lagrangian coordinates) and the other set for the deformed body (Eulerian coordinates) [37]. The deformation of a point is described by the relation of the coordinates of the same material point in the undeformed and deformed states. Let (X, Y) represent the Lagrangian coordinates, and (X^*, Y^*) the Eulerian coordinates. I use (x, y) to show the undeformed position of the point and (x^*, y^*) as the deformed position of the point as shown in Fig. (2.2). Then, a displacement of the point is defined as $q_1(x, t) = x^* - x$ and $q_2(x, t) = y^* - y$. These may be expressed in either set of the coordinates and hence the whole problem may be formulated in terms of one or the other set of coordinates. In this thesis the Lagrangian representation is chosen, so that the coordinate of a point always refers to the undeformed body which is represented by X . The undeformed and deformed infinitesimal element of the beam is drawn. 'A' is the material point of the beam in its undeformed state and 'A*' is the material point in deformed state.

According to Fig. (2.2)

$$x^* = x + q_1, \quad y^* = y + q_2 \quad (2.7)$$

For a beam with initial undeformed position overlapping the X -axis and experiencing motion in the (X, Y) plane $Y = 0$. Hence

$$x^* = x + q_1, \quad y^* = q_2 \quad \text{or} : dx^* = dx + dq_1, \quad dy^* = dq_2 \quad (2.8)$$

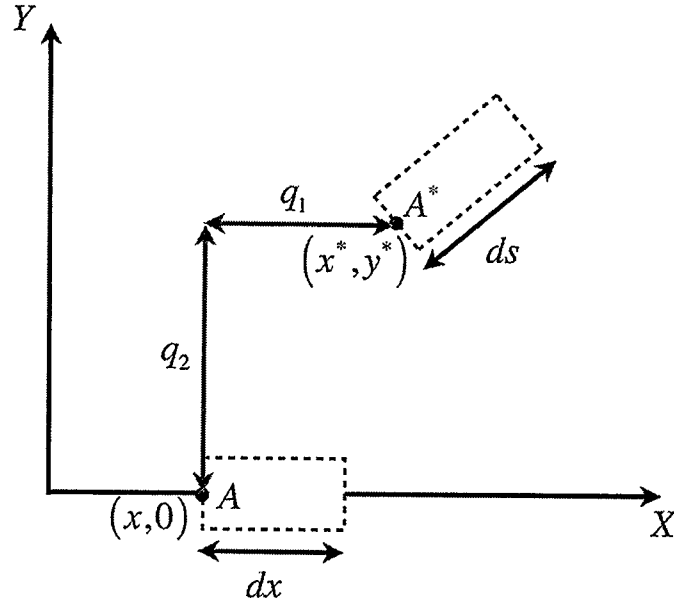


Figure 2.2: An element of the beam before and after deformation

2.3.2 Basic Relationships

An important variable for solving the beam problem is strain of the beam. The elongation of an infinitesimal element of the beam is defined as

$$e = ds - dx \quad (2.9)$$

where ds is the length of the infinitesimal element after deformation (see Fig. (2.2) and (2.3)). The strain of this element is

$$\epsilon(x) = \frac{e}{dx} = \frac{ds}{dx} - 1 \quad (2.10)$$

From Figs. (2.2) and (2.3) it follows that

$$ds = \sqrt{(dx^*)^2 + (dy^*)^2} \quad (2.11)$$

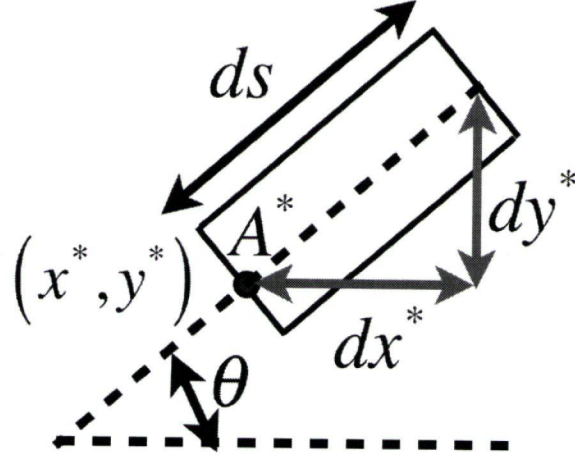


Figure 2.3: Infinitesimal element of the beam

Furthermore, using Eq. (2.8) I have

$$ds = \sqrt{(dx + dq_1)^2 + (dq_2)^2} = \sqrt{(1 + q_{1,x})^2 + q_{2,x}^2} dx \quad (2.12)$$

where $q_{1,x} \equiv \frac{dq_1}{dx}$ and $q_{2,x} \equiv \frac{dq_2}{dx}$. Finally, from Eq. (2.10) and (2.12), the strain is defined as a function of the independent variables

$$\epsilon(x) = \sqrt{(dx + dq_1)^2 + (dq_2)^2} - dx = \sqrt{(1 + q_{1,x})^2 + (q_{2,x})^2} - 1 \quad (2.13)$$

Two additional equations are readily derived by inspecting Figs. (2.2) and (2.3) and employing the equations derived up to now. They will be useful when solving the beam problem either by using Lagrangian or Newtonian framework. They are

$$\cos \theta = \frac{dx^*}{ds} = \frac{1 + q_{1,x}}{\frac{ds}{dx}} = \frac{1 + q_{1,x}}{\sqrt{(1 + q_{1,x})^2 + (q_{2,x})^2}} = \frac{1 + q_{1,x}}{1 + \epsilon} \quad (2.14)$$

and

$$\sin \theta = \frac{dy^*}{ds} = \frac{\frac{dq_2}{dx}}{\frac{ds}{dx}} = \frac{q_{2,x}}{\sqrt{(1 + q_{1,x})^2 + (q_{2,x})^2}} = \frac{q_{2,x}}{1 + \epsilon} \quad (2.15)$$

2.3.3 Beam Curvature

The curvature of a planar curve is defined as [1]

$$\kappa(x) = \frac{d\theta}{ds} \quad (2.16)$$

Where θ is the slope angle of the tangent at any point on the curve, and s is the arc length of the curve measured from an arbitrary starting point. From the geometry of the beam problem defined in Fig. (2.3) and by using the expression for y^* , Eq. (2.8), and ds , Eq. (2.12), I have

$$\theta(x) = \arcsin \frac{dy^*}{ds} = \arcsin \frac{q_{2,x}}{\sqrt{(1 + q_{1,x})^2 + (q_{2,x})^2}} \quad (2.17)$$

Taking derivative of the above equation with respect to x yields

$$\frac{d\theta}{dx} = \frac{(1 + q_{1,x})q_{2,xx} - q_{1,xx}q_{2,x}}{[(1 + q_{1,x})^2 + (q_{2,x})^2]^{\frac{3}{2}}} \quad (2.18)$$

Substituting Eq. (2.11) and (2.18) into Eq. (2.16) yields

$$\kappa(x) = \frac{(1 + q_{1,x})q_{2,xx} - q_{1,xx}q_{2,x}}{[(1 + q_{1,x})^2 + (q_{2,x})^2]^{\frac{3}{2}}} \quad (2.19)$$

The above equation is the accurate, nonlinear expression of the beam curvature. Henceforth I consider two specific cases, which correspond to the distinctive types of beam constraints.

Case 1: $q_1(x) = 0$

No axial displacement of the elements of the beam take place. This case typically exists when both ends of the beams have either the "fixed" or "pinned" constraints and their relative distance in the axial direction remains constant regardless of the transverse shape. The expression for strain and curvature becomes

$$\epsilon_1(x) = \sqrt{1 + (q_{2,x})^2} - 1 \quad (2.20)$$

$$\kappa_1(x) = \frac{q_{2,xx}}{[1 + (q_{2,x})^2]^{\frac{3}{2}}} \quad (2.21)$$

Case 2: $\epsilon(x) = 0$

Inextensible beams-this case typically exists when at least one end of the beam has the "free" or "guided" constraint. According to Eq. (2.13) the axial displacement is a function of the transverse shape $q_2(x)$

$$q_{1,x} = \sqrt{1 - (q_{2,x})^2} - 1 \quad (2.22)$$

and a simplified expression for curvature is obtained

$$\kappa_2(x) = \frac{q_{2,xx}}{\sqrt{1 - (q_{2,x})^2}} \quad (2.23)$$

Note that all the above derived equations are in Lagrangian coordinates, for a curve defined by $y^*(x^*)$ (Eulerian description), one has the familiar expression of curvature

$$\kappa(x^*) = \frac{\frac{\partial^2 y^*}{\partial x^{*2}}}{[1 + (\frac{\partial y^*}{\partial x^*})^2]^{\frac{3}{2}}} \quad (2.24)$$

2.3.4 Constitutive Equations

For a linearly elastic material the following two uncoupled constitutive equations may be used. The first is [16]

$$P = EA\epsilon \quad (2.25)$$

where P is the component of internal force in the direction of the beam axis, E is Young's modulus, A is the cross-sectional area and ϵ is the axial strain. The second constitutive equation, that connects the bending moment M with the curvature of the beam axis in the deformed state, is [16]

$$M = -EI \frac{d\theta}{dx} = -EI(1 + \epsilon)\kappa \quad (2.26)$$

2.4 Deriving the Equation of Beam Motion Using Lagrangian mechanics

The derivations in this section are based on the Hamilton's minimum action principle. Here the action is defined as [10]

$$\int_{t_1}^{t_2} (T - V + W_{nc}) dt \quad (2.27)$$

Where T is the kinetic energy, V is the potential energy and W_{nc} is the work of the non-conservative forces.

2.4.1 Kinetic Energy

The kinetic energy of the differential element under consideration is given by

$$dT = \frac{1}{2}\rho [(q_{1,t})^2 + (q_{2,t} + w_t)^2 + k_1^2\theta_t^2] dx \quad (2.28)$$

where $q_{1,t} \equiv \frac{\partial q_1}{\partial t}$, $q_{2,t} \equiv \frac{\partial q_2}{\partial t}$, $\theta_t \equiv \frac{\partial \theta}{\partial t}$ and $w_t \equiv \frac{\partial w}{\partial t}$. ρ is the mass density per length of the beam, k_1 is the mass radius of gyration of a section of the beam about the axis through the center of gravity perpendicular to the plane of motion. w is the displacement of the base in vertical direction. Integrating the above equation over the length of the beam yields

$$T(q_1, q_2) = \frac{1}{2}\rho \int_0^L [(q_{1,t})^2 + (q_{2,t} + w_t)^2 + k_1^2\theta_t^2] dx \quad (2.29)$$

2.4.2 Potential Energy

The total potential energy of the beam can be defined in terms of the strain energy and the work done by conservative forces. The potential strain energy consists of two components: the elastic strain energy due to axial stress and the elastic energy in pure bending, which are [16]

$$V_a = \int_0^L P \epsilon dx \quad (2.30)$$

and

$$V_b = \int_0^L M \frac{d\theta}{dx} dx \quad (2.31)$$

The only conservative force present on the system is the external axial force P_0 . The corresponding work done is

$$W_c = P_0 q_1(L) \quad (2.32)$$

or

$$W_c = \int_0^L P_0 q_{1,x} dx \quad (2.33)$$

since $q_1(0) = 0$.

2.4.3 Work of Nonconservative Forces

A non-conservative force acting on the beam in this research is the distributed viscous damping force. The work done by this force is computed as

$$W_{nc} = \int_0^L c_d q_{2,t} dx \quad (2.34)$$

where c_d is the damping coefficient per unit length of the beam.

2.5 Equations of Motion

Substituting the kinetic energy expression, Eq. (2.29), and the potential energy, Eqs. (2.30) and (2.31) into (2.27) I get

$$I(q_1, q_2) = \int_{t_1}^{t_2} \int_0^L F(.) dx dt \quad (2.35)$$

where

$$F(.) = \frac{1}{2} \rho [(q_{1,t})^2 + (q_{2,t} + w_t)^2 + k_1^2 \theta_t^2] - \left[M \frac{d\theta}{dx} + P \epsilon \right] + P_0 q_{1,x} - c_d q_{2,t} \quad (2.36)$$

By substituting the above equation into the Euler-Lagrange equation obtained from the calculus of variations, Eq. (2.6) one can get the two sets of partial differential equations of motion in terms of q_1 and q_2 .

2.6 Derivations Based on the Newtonian Framework

Alternatively, the beam equations can be derived also based on the Newtonian framework. Consider the free body diagram of an element of the beam shown in Fig. (2.4). In this figure $P \equiv P(x, t)$ is the total axial force, $Q \equiv Q(x, t)$ is the shear force and $M \equiv M(x, t)$ is the moment acting on the element. q is the distributed damping force. The second Newton's law for force components in horizontal (X) and vertical (Y) direction yields respectively

$$\rho (q_{2,tt} + w_{tt}) dx = (P + dP) \cos(\theta + d\theta) - P \cos \theta - (Q + dQ) \sin(\theta + d\theta) + Q \sin \theta - c_d q_{2,t} \quad (2.37)$$

and

$$\rho q_{1,tt} dx = (P + dP) \sin(\theta + d\theta) - P \sin \theta + (Q + dQ) \cos(\theta + d\theta) - Q \cos \theta \quad (2.38)$$

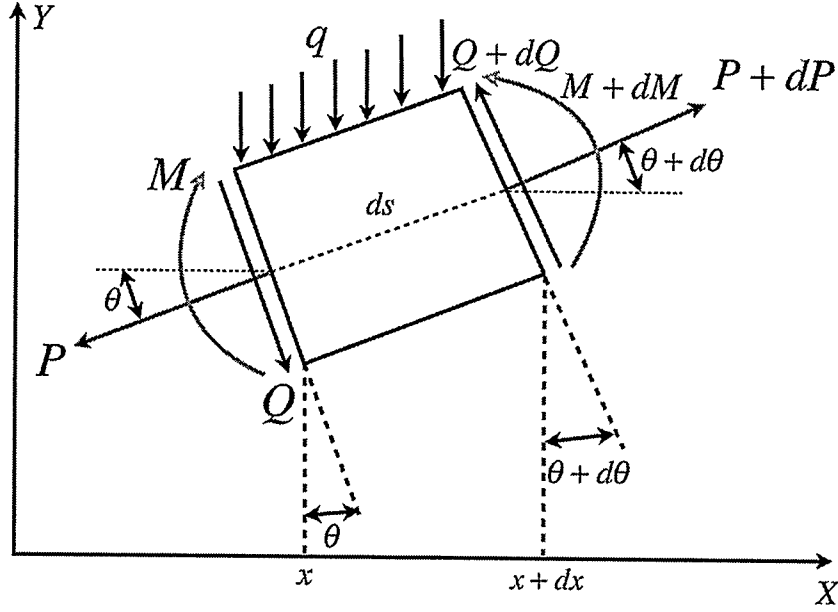


Figure 2.4: Free body diagram for an element of the beam

Taylor series expansion of the functions $\sin \theta$ and $\cos \theta$

$$\begin{aligned}\sin(\theta + d\theta) &= \sin \theta + \cos \theta d\theta + \mathcal{O}(d\theta)^2 \\ \cos(\theta + d\theta) &= \cos \theta - \sin \theta d\theta + \mathcal{O}(d\theta)^2\end{aligned}\quad (2.39)$$

allows to rewrite Eq. (2.37) and (2.38) as

$$\rho q_{1,tt} = -P \sin \theta \frac{d\theta}{dx} + \cos \theta \frac{dP}{dx} - Q \cos \theta \frac{d\theta}{dx} - \sin \theta \frac{dQ}{dx} \quad (2.40)$$

$$\rho q_{2,tt} = P \cos \theta \frac{d\theta}{dx} + \sin \theta \frac{dP}{dx} - Q \sin \theta \frac{d\theta}{dx} + \cos \theta \frac{dQ}{dx} \quad (2.41)$$

Following the Euler-Bernouli beam model, I add the moment equation

$$-(M + dM) + M + (Q + dQ)ds = \rho k_1^2 \theta_{tt} \quad (2.42)$$

Simplifying and ignoring the infinitesimals of higher order [30] yields

$$Q = \left(\frac{dM}{dx} + \rho k_1^2 \theta_{tt} \right) \frac{dx}{ds} \quad (2.43)$$

Using Eqs. (2.12) and (2.13) I can rewrite the above equation as

$$Q = \left(\frac{dM}{dx} + \rho k_1^2 \theta_{tt} \right) \frac{1}{1 + \epsilon(q_1, q_2)} \quad (2.44)$$

By substituting the expressions for $\sin(\theta)$ and $\cos(\theta)$ developed earlier, Eqs. (2.14) and (2.15), and the equation for derivative of θ with respect to x , Eq. (2.18), and the moment-curvature relation, Eq. (2.26), and also the constitutive equation for the internal normal force, P , applying on the element, Eq. (2.25), and the above equation, Eq. (2.44), into Eqs. (2.40) and (2.41) one can obtain the same equations as those that can be derived by employing the Lagrangian framework. The derived equations will be in terms of the two generalized coordinates, q_1 and q_2 .

Another approach, which is proposed in [5], is to find a system of equations that finally describe the motion of a beam in terms of other two independent variables, one related to axial displacement q_1 and the other one related to θ . The advantage is that for the static case the equations reduce to a simple second order ODE in terms of θ , and the exact solution of this ODE can be expressed in terms of elliptical integrals [16]. Note that as shown in Eq. (2.17), θ is a function of q_1 and q_2 when the Euler-Bernoulli hypothesis is used, whereas in the Timoshenko hypothesis, where shear strain exists, three independent functions, e.g. q_1 , q_2 and θ are needed to define the motion of the beam. Following the procedure proposed in [5] one can draw the free body diagram of the beam as shown in Fig. (2.5).

Here H and V are the X and Y component of the internal force and q is the damping force ($q = c_d q_{2,t} dx$). The following equations can be derived from the free

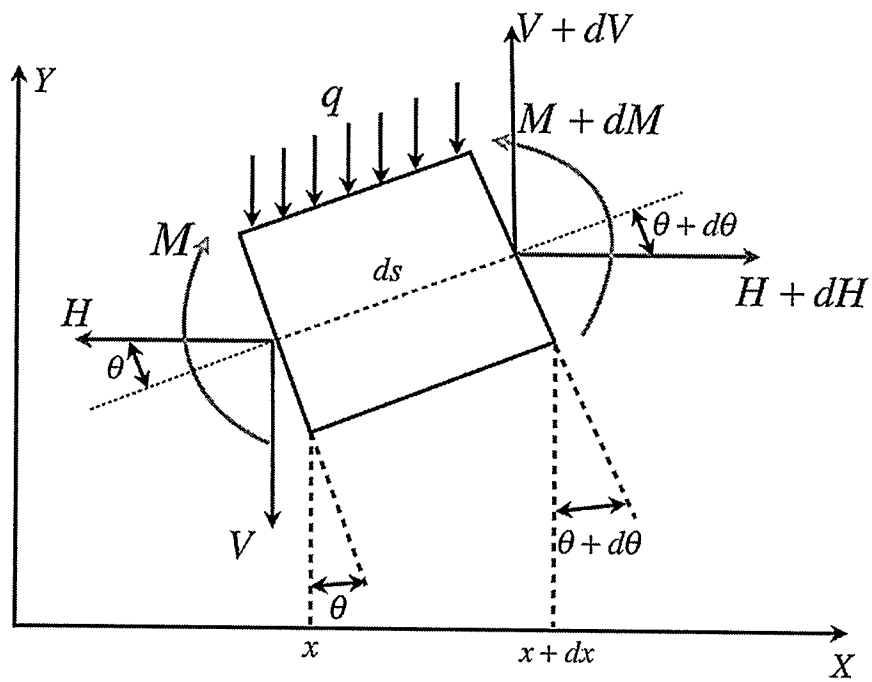


Figure 2.5: Alternative free body diagram for the beam element

body diagram

$$\begin{aligned}
 \rho q_{1,tt} &= H_x \\
 \rho q_{2,tt} &= V_x - c_d q_{2,t} - \rho w_{tt} \\
 M_x &= V \cos \theta \frac{ds}{dx} - H \sin \theta \frac{ds}{dx} - \rho k_1^2 \theta_{tt}
 \end{aligned} \tag{2.45}$$

where $(\cdot)_x \equiv \frac{\partial(\cdot)}{\partial x}$. The last equation above can be written as (See Eq. (2.10))

$$M_x = V \cos \theta (1 + \epsilon) - H \sin \theta (1 + \epsilon) - \rho k_1^2 \theta_{tt} \tag{2.46}$$

Furthermore, the normal force P can be expressed in terms of H , V and θ . Using the constitutive equation for P , Eq. (2.25), yields

$$\epsilon = \frac{H \cos \theta + V \sin \theta}{EA} \tag{2.47}$$

Also using Eqs. (2.14) and (2.15) and the above equation I get

$$q_{1,x} = \left(1 + \frac{H \cos \theta + V \sin \theta}{EA}\right) \cos \theta - 1 \tag{2.48}$$

and

$$q_{2,x} = \left(1 + \frac{H \cos \theta + V \sin \theta}{EA}\right) \sin \theta \tag{2.49}$$

In summary I have the following system of equations

$$\begin{aligned}
 H_x &= \rho q_{1,tt}, \\
 V_x &= \rho q_{2,tt} + c_d q_{2,t} + \rho w_{tt}, \\
 M_x &= \left(1 + \frac{H \cos \theta + V \sin \theta}{EA}\right) (V \cos \theta - H \sin \theta) - \rho k_1^2 \theta_{tt}, \\
 q_{1,x} &= \left(1 + \frac{H \cos \theta + V \sin \theta}{EA}\right) \cos \theta - 1, \\
 q_{2,x} &= \left(1 + \frac{H \cos \theta + V \sin \theta}{EA}\right) \sin \theta, \\
 \theta_x &= -\frac{M}{EI}
 \end{aligned} \tag{2.50}$$

The boundary conditions for the beam under study are

$$\begin{aligned}
q_1(t, x = 0) &= 0, & H(t, x = L) &= -P_0, \\
M(t, x = 0) &= 0, & M(t, x = L) &= 0, \\
q_2(t, x = 0) &= 0, & q_2(t, x = L) &= 0
\end{aligned} \tag{2.51}$$

Before I consider the specific aspects of the derived equations, the utility of non-dimensionalizing the equations is mentioned. Non-dimensionalization is useful because it reduces the number of parameters and allows a more consistent comparison of behavior. One can introduce the non-dimensional quantities as

$$\begin{aligned}
\mathcal{H} &= \frac{(H + P_0)L^2}{EI}, & \mathcal{V} &= \frac{VL^2}{EI}, & \mathcal{M} &= \frac{ML}{EI}, & u &= \frac{q_1 + \frac{P_0x}{EA}}{L}, & \gamma &= \frac{k_1}{L}, \\
\mu &= \sqrt{\frac{AL^2}{I}}, & v &= \frac{q_2}{L}, & \lambda &= \frac{P_0L^2}{EI}, & \xi &= x/L, & \tau &= t\sqrt{\frac{EI}{\rho L^4}}, \\
C &= c_d\sqrt{\frac{L^2}{\rho EI}}, & \Omega &= \omega\sqrt{\frac{\rho L^4}{EI}}, & \mathcal{A} &= \frac{AL^3}{EI}
\end{aligned} \tag{2.52}$$

Here Ω and \mathcal{A} are the non-dimensionalized frequency and amplitude of vibration and w is the base excitation which is assumed to be harmonic. ($w_{tt} = \mathbf{A} \cos(\omega t)$).

Substituting the non-dimensionalized quantities into Eq. (2.50) yields

$$\begin{aligned}
\mathcal{H}_\xi &= u_{\tau\tau}, \\
\mathcal{V}_\xi &= v_{\tau\tau} + Cv_\tau + \mathcal{A} \cos(\Omega\tau), \\
\mathcal{M}_\xi &= \mathcal{V} \left(1 + \frac{(-\lambda + \mathcal{H}) \cos \theta + \mathcal{V} \sin \theta}{\mu^2} \right) \cos \theta \\
&\quad - (-\lambda + \mathcal{H}) \left(1 + \frac{(-\lambda + \mathcal{H}) \cos \theta + \mathcal{V} \sin \theta}{\mu^2} \right) \sin \theta - \gamma^2 \theta_{\tau\tau}, \\
u_\xi &= \left(1 + \frac{(-\lambda + \mathcal{H}) \cos \theta + \mathcal{V} \sin \theta}{\mu^2} \right) \cos \theta - \left(1 - \frac{\lambda}{\mu^2} \right), \\
v_\xi &= \left(1 + \frac{(-\lambda + \mathcal{H}) \cos \theta + \mathcal{V} \sin \theta}{\mu^2} \right) \sin \theta, \\
\theta_\xi &= -\mathcal{M}
\end{aligned} \tag{2.53}$$

And the boundary conditions change to

$$\begin{aligned}
 u(\tau, \xi = 0) = 0, \quad \mathcal{H}(\tau, \xi = 1) = 0, \\
 \mathcal{M}(\tau, \xi = 0) = 0, \quad \mathcal{M}(\tau, \xi = 1) = 0, \\
 v(\tau, \xi = 0) = 0, \quad v(\tau, \xi = 1) = 0, \quad \mathcal{V}(\tau, \xi = 1) = 0
 \end{aligned} \tag{2.54}$$

The system of Eqs. (2.53) with the associated boundary conditions, Eqs. (2.54), and given initial conditions describe the motion of an extensible 2D Euler-Bernoulli beam. The damping forces, excitation forces, rotary inertia terms and axial displacement of the beam as well as transverse displacement are included in this system of equations. Similar results have been obtained in [5] for the free vibration of undamped extensible beam. Note that the above equations are exact, i.e. they contain no approximation whatsoever concerning the magnitude of displacement. The only assumptions here are that (i) normal sections remain plane, undistorted and normal to the axis of the beam after deformation (shear effects are neglected) and (ii) the two constitutive equations, Eqs. (2.25) and (2.26), are adopted for the internal normal axial force and the bending moment.

2.7 Previous Derivations

The vibration of an elastic beam were studied with various degrees of approximations for a long time. Here I present summarized derivations of the equations of beam motion for two important assumptions which have been used frequently for studying the nonlinear behavior of beams, namely the equations for (i) *inextensible beam* and (ii) *1D extensible beam*.

Case 1: 1D extensible beam

In this case the beam is assumed to experience midplane stretching, but the axial motion and rotary inertia terms are ignored. Here I follow the procedure presented in [7]. The average strain assumption is applied for calculation of the potential energy due to the axial forces. The average strain ($\bar{\epsilon}$) for a beam is

$$\bar{\epsilon} = \frac{\Delta}{L} \quad (2.55)$$

where Δ is the total elongation of the beam and has the following relationship with the strain (ϵ_1)

$$\Delta = \int_0^L \epsilon_1 dx \quad (2.56)$$

The strain of the beam is given by Eq. (2.20) and it is approximated as

$$\epsilon_1(x) = \left(\sqrt{1 + (q_{2,x})^2} - 1 \right) \simeq \frac{1}{2} (q_{2,x})^2 \quad (2.57)$$

Hence, the total elongation of the beam is

$$\Delta = \int_0^L \epsilon_1 dx = \frac{1}{2} \int_0^L q_{2,x}^2 dx \quad (2.58)$$

Considering the average strain assumption, the potential energy due to an external axial force (P_0) will be equal to the work done by the axial force multiplied by the displacement Δ , which is the total elongation of the beam

$$V_{a_0} = -P_0 \Delta \quad (2.59)$$

The potential energy due to internal axial force is

$$V_{a_i} = \frac{1}{2} \mathcal{J} \Delta \quad (2.60)$$

where (\mathcal{J}) is the internal axial force due to elongation of the beam

$$\mathcal{J} = EA\bar{\epsilon} = \frac{EA}{L} \Delta = \frac{EA}{L} \int_0^L \epsilon_1 dx \quad (2.61)$$

Hence, for an axial external compressive applied force, the potential energy due to axial stress is

$$\begin{aligned} V_a = V_{a_0} + V_{a_1} &= - \left(P_0 - \frac{EA}{2L} \int_0^L \epsilon_1 dx \right) \int_0^L \epsilon_1 dx \\ &= - \left(P_0 - \frac{EA}{2L} \Delta \right) \Delta \end{aligned} \quad (2.62)$$

Substituting Eq. (2.58), one gets

$$V_a(q_2) = -\frac{1}{2} \left(P_0 - \frac{EA}{4L} \int_0^L (q_{2,x})^2 dx \right) \int_0^L (q_{2,x})^2 dx \quad (2.63)$$

The beam curvature for extensible beam (Eq. (2.21)) can be approximated by using the binomial series

$$\kappa_1 \simeq q_{2,xx} \quad (2.64)$$

So, the relationship between the beam curvature and bending moment can be expressed as

$$M = EI\kappa_1 \simeq EIq_{2,xx} \quad (2.65)$$

The potential energy of bending is

$$V_b(q_2) = \frac{1}{2} EI \int_L q_{2,xx}^2 dx \quad (2.66)$$

By using Eqs. (2.63), (2.66), considering the damping force and Lagrangian framework, one can derive the equation describing the motion of a 1D extensible beam as [7]

$$\rho q_{2,tt} + c_d q_{2,t} + A \cos(\omega t) + EI q_{2,xxxx} + \left(P_0 - \frac{EA}{2L} \int_0^L q_{2,x}^2 dx \right) q_{2,xx} = 0 \quad (2.67)$$

with the following boundary condition for a simply supported beam

$$\begin{aligned} q_2(x=0, t) &= q_2(x=L, t) = 0 \\ q_{2,xx}(x=0, t) &= q_{2,xx}(x=L, t) = 0 \end{aligned} \quad (2.68)$$

Note that due to ignoring the q_1 generalized coordinate, only one differential equation has been obtained. Again, by introducing the following non-dimensionalized quantities

$$\begin{aligned} \mu &= \sqrt{\frac{AL^2}{I}}, & v &= \frac{q_2}{L}, & \lambda &= \frac{P_0L^2}{EI}, & \xi &= x/L, & \tau &= t\sqrt{\frac{EI}{\rho L^4}}, \\ C &= c_d\sqrt{\frac{L^2}{\rho EI}}, & \Omega &= \omega\sqrt{\frac{\rho L^4}{EI}}, & \mathcal{A} &= \frac{AL^3}{EI} \end{aligned} \quad (2.69)$$

one can rewrite the 1D extensible beam equation as

$$v_{\tau\tau} + Cv_{\tau} + \mathcal{A}\cos(\Omega t) + v_{\xi\xi\xi\xi} + \lambda v_{\xi\xi} - \frac{1}{2}\mu^2 v_{\xi\xi} \int_0^1 v_{\xi}^2 d\xi = 0 \quad (2.70)$$

and the boundary conditions change to

$$\begin{aligned} v(\xi = 0, \tau) &= v(\xi = 1, \tau) = 0, \\ v_{\xi\xi}(\xi = 0, \tau) &= v_{\xi\xi}(\xi = 1, \tau) = 0 \end{aligned} \quad (2.71)$$

Case 2: Inextensible beam ($\epsilon = 0$)

In [28] the equation of motion for an inextensible beam is derived, with a small error in their derivation which will be discussed at the end of this section. As stated earlier, under the inextensibility condition, Eq. (2.22), q_1 is a function of q_2 . This relationship is simplified as follows [28]

$$q_{1,x} \simeq -\frac{1}{2}q_{2,x}^2 \quad (2.72)$$

Hence, the potential energy due to axial force, Eq. (2.32) can be expressed as

$$V_a(q_2) = -P_0 \int_0^L \frac{1}{2}q_{2,x}^2 dx \quad (2.73)$$

The expression for the bending moment of an inextensible beam, Eq. (2.26), becomes

$$M = EI\kappa_2 \quad (2.74)$$

where κ_2 is the curvature of an inextensible beam. As discussed before in section 2.3.3, the curvature expression for the inextensible beam is Eq. (2.23) and after expansion, it is written as

$$\kappa_2 \simeq q_{2,xx} \left(1 + \frac{1}{2}q_{2,x}^2 \right) \quad (2.75)$$

The energy due to bending is written as

$$V_b = \frac{1}{2}EI \int_L \kappa_2^2 dx = \frac{1}{2}EI \int_L \left(q_{2,xx}^2 \left(1 + q_{2,x}^2 + \frac{1}{4}q_{2,x}^4 \right) \right) dx \quad (2.76)$$

Using Eq. (2.76) and (2.73), the expression for kinetic energy and damping force, and using the Lagrangian mechanics, one can obtain the equation for motion of an inextensible beam in terms of q_2 [28]

$$\begin{aligned} \rho q_{2,tt} + c_d q_{2,t} + \mathbf{A} \cos(\omega t) + EI q_{2,xx} \left(q_{2,xx}^2 \left(1 + \frac{3}{2}q_{2,x}^2 \right) + 4q_{2,x}q_{2,xxx} \left(1 + \frac{1}{2}q_{2,x}^2 \right) \right) \\ + EI q_{2,xxxx} \left(1 + q_{2,x}^2 + \frac{1}{4}q_{2,x}^4 \right) + P_0 q_{2,xx} = 0 \end{aligned} \quad (2.77)$$

Although Eq. (2.76) is obtained from Eq. (2.75), but the order of magnitude of the neglected terms in these two equations are not the same. In Eq. (2.75) the terms with order higher than $q_{2,x}^3$ are ignored, but in Eq. (2.76) the $q_{2,x}^4$ term exists. If one is interested to keep up to fourth order terms in (2.76), then Eq. (2.75) should include these terms as well

$$\kappa \simeq q_{2,xx} \left(1 + \frac{1}{2}q_{2,x}^2 + \frac{3}{8}q_{2,x}^4 \right) + \dots \quad (2.78)$$

Now by inserting Eq. (2.78) into (2.76) I get the correct equation for V_b

$$V_b(q_2) = \frac{1}{2}EI \int_L (q_{2,xx}^2 (1 + q_{2,x}^2 + q_{2,x}^4)) dx \quad (2.79)$$

Finally using the corrected form of V_b yields

$$\begin{aligned} \rho q_{2,tt} + c_d q_{2,t} + A \cos(\omega t) + EI q_{2,xx} (q_{2,xx}^2 (1 + 6q_{2,x}^2) + 4q_{2,x} q_{2,xxx} (1 + 2q_{2,x}^2)) \\ + EI q_{2,xxxx} (1 + q_{2,x}^2 + q_{2,x}^4) + P_0 q_{2,xx} = 0 \end{aligned} \quad (2.80)$$

with the boundary conditions given by Eq. (2.68).

the non-dimensionaized format of the inextensible beam equation is

$$v_{\tau\tau} + C v_{\tau} + \mathcal{A} \cos(\Omega t) + v_{\xi\xi} (v_{\xi\xi}^2 (1 + 6v_{\xi}^2) + 4v_{\xi} v_{\xi\xi\xi} (1 + 2v_{\xi}^2)) + v_{\xi\xi\xi\xi} (1 + v_{\xi}^2 + v_{\xi}^4) + \lambda v_{\xi\xi} = 0 \quad (2.81)$$

with the boundary conditions defined by Eq. (2.71).

Chapter 3

Static Solution

The goal in this chapter is to derive the equations of a 2D elastic extensible beam for the static case, find the buckling load and the equilibrium paths when the beam buckles. The results are also compared with the static behavior of the 1D extensible and inextensible beam.

3.1 Static Equations

The general equations of motion for a 2D extensible beam is derived in Chapter 2, Eq. (2.53). For the static case, these equations are

$$\begin{aligned}
 \mathcal{H}_\xi &= 0, \\
 \mathcal{V}_\xi &= 0, \\
 \mathcal{M}_\xi &= \mathcal{V} \left(1 + \frac{(-\lambda + \mathcal{H}) \cos \theta + \mathcal{V} \sin \theta}{\mu^2} \right) \cos \theta \\
 &\quad - (-\lambda + \mathcal{H}) \left(1 + \frac{(-\lambda + \mathcal{H}) \cos \theta + \mathcal{V} \sin \theta}{\mu^2} \right) \sin \theta - \gamma^2 \theta_{\tau\tau}, \\
 u_\xi &= \left(1 + \frac{(-\lambda + \mathcal{H}) \cos \theta + \mathcal{V} \sin \theta}{\mu^2} \right) \cos \theta - \left(1 - \frac{\lambda}{\mu^2} \right), \\
 v_\xi &= \left(1 + \frac{(-\lambda + \mathcal{H}) \cos \theta + \mathcal{V} \sin \theta}{\mu^2} \right) \sin \theta, \\
 \theta_\xi &= -\mathcal{M}
 \end{aligned} \tag{3.1}$$

with the boundary conditions

$$\begin{aligned}
 \mathcal{H}(\xi = 1) &= 0, & \mathcal{V}(\xi = 1) &= v(\xi = 1) = 0, \\
 \mathcal{M}(\xi = 0) &= 0, & \mathcal{M}(\xi = 1) &= 0, \\
 u(\xi = 0) &= 0, & v(\xi = 0) &= 0
 \end{aligned} \tag{3.2}$$

The first two equations with the associated boundary conditions yield

$$\begin{aligned}\mathcal{H}(\xi) &= 0, \\ \mathcal{V}(\xi) &= 0\end{aligned}\tag{3.3}$$

Substituting the above equations into Eq. (3.1) results

$$\mathcal{M}_\xi = \lambda \left(1 - \frac{\lambda}{\mu^2} \cos \theta\right) \sin \theta\tag{3.4}$$

$$u_\xi = \left(1 - \frac{\lambda}{\mu^2} \cos \theta\right) \cos \theta - \left(1 - \frac{\lambda}{\mu^2}\right)\tag{3.5}$$

$$v_\xi = \left(1 - \frac{\lambda}{\mu^2} \cos \theta\right) \sin \theta\tag{3.6}$$

$$\theta_\xi = -\mathcal{M}\tag{3.7}$$

By combining Eqs. (3.4) and (3.7) obtains

$$\theta_{\xi\xi} + \lambda \left(1 - \frac{\lambda}{\mu^2} \cos \theta\right) \sin \theta = 0\tag{3.8}$$

From Eq. (3.2) the boundary conditions for the above equation are

$$\theta_\xi(\xi = 0) = 0, \quad \theta_\xi(\xi = 1) = 0\tag{3.9}$$

To summarize, the static problem is defined by a second order ordinary differential equation, Eq. (3.8), with the above boundary conditions. Equations (3.5) and (3.6) relates the axial and transversal displacement to θ . Our interest in the static case is to find the transversal displacement. Comparing Eq. (3.8) and (3.6) yields

$$\theta_{\xi\xi} + \lambda v_\xi = 0\tag{3.10}$$

So

$$v(\xi) = -\frac{1}{\lambda}\theta_\xi + c_1 \quad (3.11)$$

At the beam ends both the transversal deflection and the moment are zero, so that $c_1 = 0$. Identical results have been obtained in [16] with a different technique (and notations). The goal is now to find a slope $\theta(\xi)$ such that it corresponds to an equilibrium deformed position of the beam. Once $\theta(\xi)$ is found, Eq. (3.11) can be used to compute the transversal displacement. It can be noticed that a trivial solution $\theta(\xi) = 0$ exists, i.e. the fundamental solution, however what is interesting here is to find a nontrivial solution corresponding to a deformed equilibrium position of the beam.

Static Equation, Alternative Derivations

The equation for the inextensible and 1D extensible beam can be easily obtained by dropping the inertia and damping terms in Eqs. (2.81) and (2.70) respectively. One can write the 1D extensible beam static equation as

$$v_{\xi\xi\xi\xi} + \lambda v_{\xi\xi} - \frac{1}{2}\mu^2 v_{\xi\xi} \int_0^1 v_\xi^2 d\xi = 0 \quad (3.12)$$

and the boundary conditions

$$\begin{aligned} v(\xi = 0) &= v(\xi = 1) = 0, \\ v_{\xi\xi}(\xi = 0) &= v_{\xi\xi}(\xi = 1) = 0 \end{aligned} \quad (3.13)$$

For the inextensible beam, the following equation is obtained

$$v_{\xi\xi}(v_{\xi\xi}^2(1 + 6v_\xi^2) + 4v_\xi v_{\xi\xi\xi}(1 + 2v_\xi^2)) + v_{\xi\xi\xi\xi}(1 + v_\xi^2 + v_\xi^4) + \lambda v_{\xi\xi} = 0 \quad (3.14)$$

with the (same) boundary conditions (as) defined in Eq. (3.13).

3.1.1 The Buckling Load

Before discussion on the nontrivial solutions for the 2D extensible beam, the properties of the fundamental solutions are studied. It turns out that it is sufficient to consider the linearized problem around $\theta = 0$ when the fundamental path is analyzed [16]. Based on this analysis one can find the buckling load and eigenmodes of the beam. A linearization of Eq. (3.8) yields

$$\theta_{\xi\xi} + \lambda\left(1 - \frac{\lambda}{\mu^2}\right)\theta = 0 \quad (3.15)$$

From the above equation and the associated boundary conditions, Eq. (3.9), it follows that the eigenfunctions are given as

$$\theta_n(\xi) = c_n \cos(n\pi\xi), \quad n = 1, 2, 3, \dots \quad (3.16)$$

where c_n coefficients are arbitrary. Insertion of Eq. (3.16) into Eq. (3.15) yields

$$\left((n\pi)^2 + \lambda\left(1 - \frac{\lambda}{\mu^2}\right) \right) c_n \cos(n\pi\xi) = 0 \quad (3.17)$$

Or

$$(n\pi)^2 + \lambda\left(1 - \frac{\lambda}{\mu^2}\right) = 0 \quad (3.18)$$

must hold in general. From the above equation one can find the expression for the buckling load (λ_{cr}). The solution to this second-order equations is given by

$$\lambda_{cr} = \frac{\mu^2}{2} \left(1 \pm \sqrt{1 - \frac{4n^2\pi^2}{\mu^2}} \right) \quad (3.19)$$

The above equation shows the dependency of the buckling load on the slenderness ratio of the beam, μ . Based on classical Euler-Bernoulli beam theory, either for the inextensible beam or 1D extensible beam, one can derive the expression for the buckling load as [27, 28]

$$P_{cr} = n^2 P_E \quad (3.20)$$

where

$$P_E = \frac{\pi^2 EI}{L^2} \quad (3.21)$$

is the Euler buckling load. The above equations can be rewritten in terms of the non-dimensionalized parameter λ as

$$\lambda_{cr} = n^2 \lambda_E \quad (3.22)$$

and

$$\lambda_E = \pi^2 \quad (3.23)$$

Interestingly, in contrast to the inextensible or 1D extensible case, for the 2D extensible beam only a limited number of buckling loads exist and their value depend on the slenderness of the beam [16]. Furthermore, Eq. (3.19) shows that for $n = 1$ when $\mu < 2\pi$ no real solutions (buckling loads) exist, implying that for short beams buckling never occurs. A physical interpretation of this could be that the shortening of the beam compensates the increase of the load that much that buckling never occurs [16]. In Fig. (3.1) the ratio of buckling load for 2D extensible (for $n = 1$) to λ_E versus slenderness ratio μ is plotted. This figure shows that for large values of μ , the buckling load of 2D extensible beam reaches the Euler buckling load.

3.2 Equilibrium Paths

In [16] the exact solution of Eq. (3.8) is obtained in terms of elliptic integrals. The procedure is as follows. First Eq. (3.8) is multiplied by θ_ξ , so that it becomes

$$\theta_\xi \theta_{\xi\xi} + \theta_\xi \lambda \left(1 - \frac{\lambda}{\mu^2} \cos \theta\right) \sin \theta = 0 \quad (3.24)$$

which can be written as

$$\frac{d}{d\xi} \left(\frac{1}{2} \theta_\xi^2 - \lambda \cos \theta + \frac{\lambda}{2\mu^2} \cos^2 \theta \right) = 0 \quad (3.25)$$

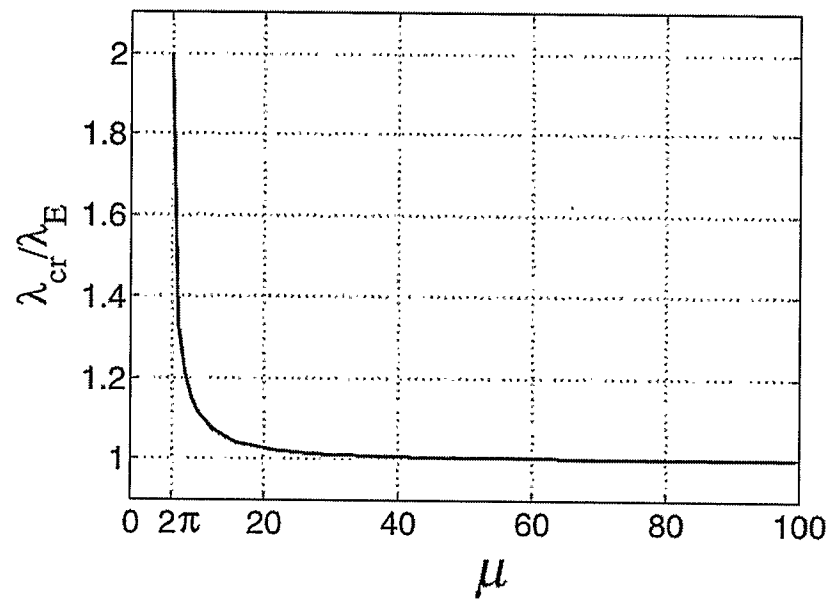


Figure 3.1: Buckling load of a 2D extensible beam

where it is immediately integrable. At the ends of a simply supported beam, θ is unknown, whereas $\theta_\xi = 0$. Integration of the above equation and letting α be the unknown slope at the ends of the beam, it follows that

$$\frac{1}{2}\theta_\xi^2 = \lambda \cos \theta - \frac{\lambda}{2\mu^2} \cos^2 \theta - \lambda \cos \alpha + \frac{\lambda}{2\mu^2} \cos^2 \alpha \quad (3.26)$$

Therefore

$$\theta_\xi = 2\sqrt{\lambda} \sqrt{(1 - e)(h^2 - \sin^2 \frac{\theta}{2}) + e(h^4 - \sin^4 \frac{\theta}{2})} \quad (3.27)$$

where the positive root is chosen and

$$\begin{aligned} e &= \frac{\lambda}{\mu^2}, \\ h &= \sin \frac{\alpha}{2} \end{aligned} \quad (3.28)$$

In order to simplify the notation, a new variable ϕ is defined as

$$\sin \phi = \frac{\sin \frac{\theta}{2}}{\sin \frac{\alpha}{2}} \quad (3.29)$$

Since it is known that θ will have $n + 1$ extreme values (See Eq. (3.16)), the new variable ϕ is expected to vary from $-\frac{\pi}{2}$ to $n\pi - \frac{\pi}{2}$ from one end of the beam to the other end. Using this variable, Eq. (3.27) can be rewritten as

$$\theta_\xi = 2h \cos \phi \sqrt{\lambda} \sqrt{1 - e + h^2 e(1 + \sin^2 \phi)} \quad (3.30)$$

The left hand side of this equation can be written as

$$\theta_\xi = \frac{d\phi}{d\xi} \frac{d\theta}{d\phi} = \phi_\xi \theta_\phi = \phi_\xi \frac{2h \cos \phi}{\sqrt{1 - h^2 \sin^2 \phi}} \quad (3.31)$$

Combining this equation with Eq. (3.30) yields

$$\phi_\xi = \sqrt{\lambda} \sqrt{(1 - h^2 \sin^2 \phi)(1 - e + h^2 e(1 + \sin^2 \phi))} \quad (3.32)$$

The above equation can be integrated to yield

$$\int_0^{\frac{\pi}{2}} \frac{d\phi}{\sqrt{(1-h^2 \sin^2 \phi)(1-e+h^2 e(1+\sin^2 \phi))}} = \frac{1}{2n} \sqrt{\lambda} \quad (3.33)$$

The above integral on the left side of equation can be reduced to an elliptic integral by the substitution of variables

$$\sin^2 \phi = \frac{(1-e+eh^2) \sin^2 \psi}{1-e+2eh^2-eh^2 \sin^2 \psi} \quad (3.34)$$

with this substitution Eq. (3.33) becomes [16]

$$\frac{\mu\sqrt{e}}{2} = \int_0^{\frac{\pi}{2}} \frac{nd\psi}{\sqrt{1-e+2eh^2-h^2(1+eh^2)\sin^2 \psi}} = \frac{n}{\sqrt{1-e+2eh^2}} K\left(h\sqrt{\frac{1+eh^2}{1-e+2eh^2}}\right) \quad (3.35)$$

Where the integral in the above equation is a complete elliptic integral of the first kind, $K(k)$ and its values are tabulated. For a given e and μ , h and hence the unknown slope at the beam ends can be calculated. Having this value as the initial condition for Eq. (3.8) the expression for $\theta(\xi)$ at equilibrium can be derived. Having this expression one can find the transversal displacement, $v(\xi)$ and hence the equilibrium path.

Equilibrium Path, Alternative Derivations

The equilibrium path for a 1D extensible and inextensible beam can be obtained from numerical solution of Eq. (3.12) and Eq. (3.14). In [27] the exact solution of Eq. (3.12) has been derived. Figure (3.2) compares the equilibrium path of 2D extensible, 1D extensible and inextensible beam for the slenderness ratio $\mu = 10$. In Fig. (3.3) the difference between the exact solution of a 2D extensible beam and 1D extensible/Inextensible beam are depicted. Results show that there is always a good match between the 2D extensible and inextensible beam results, however the 1D extensible

model is not accurate for predicting the shape of beams with large μ . By increasing μ the differences between the results of these three different models increase.

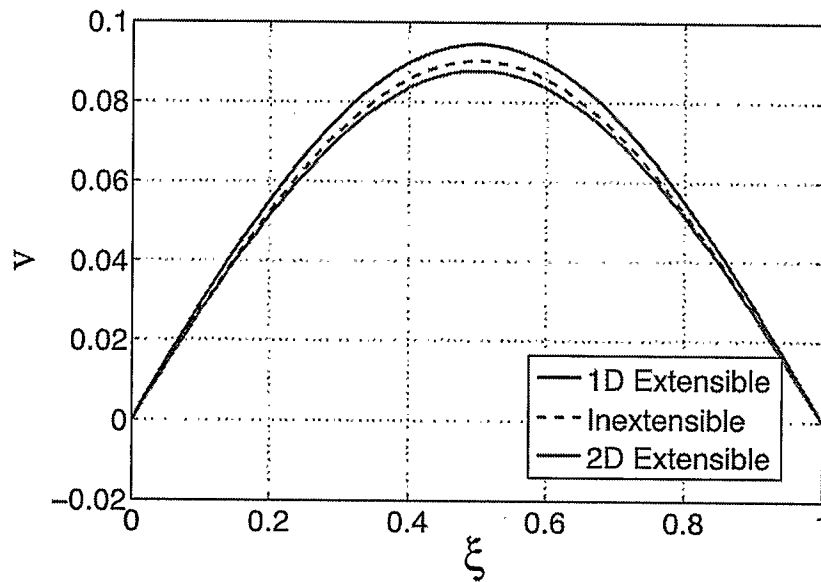


Figure 3.2: Equilibrium path for a buckled beam, $\mu = 10$, $\lambda = 1.01\lambda_{cr}$

Also in Fig. (3.4), the maximum deflection of the beam versus different axial forces, i.e. different values of λ , for $\mu = 150$ are plotted. Again the results of inextensible and 2D extensible model are very close. By increasing the external applied force the difference between results of these three models rapidly increases.

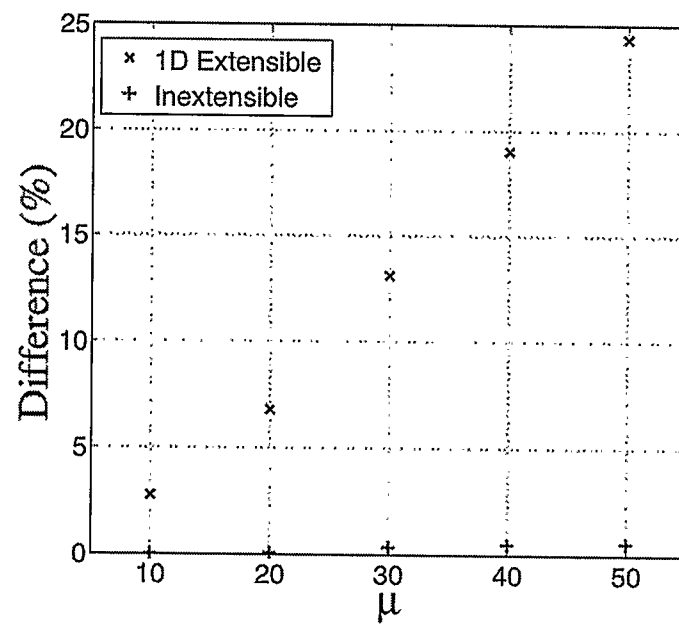


Figure 3.3: Difference between the exact solution of 2D extensible beam and (a) 1D Extensible and (b) Inextensible beam

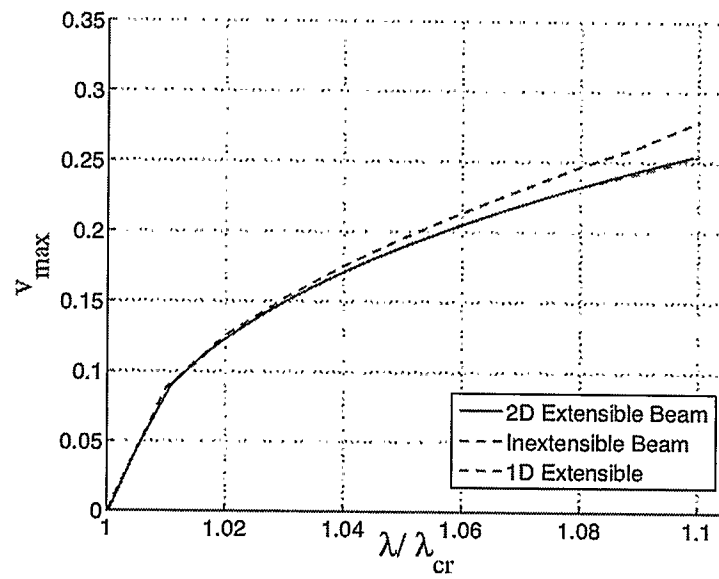


Figure 3.4: Load-paths for 2D extensible, 1D extensible and inextensible beam, $\mu = 150$

Chapter 4

Dynamic Solution

This chapter is concerned with beam dynamics. First the linearized equations of 2D extensible elastic beam are investigated. Based on the linearized equations the expressions for natural frequencies and mode shape of the beam are derived. Employing the Galerkin mode shape expansion method and expanding the non-linear terms into a Taylor series, the non-linear partial differential equations (PDEs) of motion are approximated by a set of ordinary differential equations (ODEs). The effect of higher order terms in the Taylor series expansion as well as the effect of including higher order mode shapes in Galerkin's method are studied. The same approach is employed to approximate the PDEs of 1D extensible and inextensible beam models.

4.1 Linearized Equations

The general equations describing the motion of a forced 2D extensible elastic beam with damping have been derived in Chapter 2, Eqs. (2.53) and (2.54). For small \mathcal{H} , \mathcal{V} , \mathcal{M} , u , v and θ , and for undamped free vibration of the beam ($C = 0$, $\mathcal{A} = 0$), one can linearize the non-linear equations as [5]

$$\begin{aligned}
 \mathcal{H}_\xi &= u_{\tau\tau}, & \mathcal{V}_\xi &= v_{\tau\tau}, \\
 \mathcal{M}_\xi &= \mathcal{V}\alpha - \lambda\alpha\theta - \gamma^2\theta_{\tau\tau}, & u_\xi &= \frac{\mathcal{H}}{\mu^2}, \\
 v_\xi &= \alpha\theta, & \theta_\xi &= -\mathcal{M}
 \end{aligned} \tag{4.1}$$

where

$$\alpha = 1 - \frac{\lambda}{\mu^2} \quad (4.2)$$

From Eqs. (4.1) it follows that

$$\mathcal{H}_\xi = \frac{\partial}{\partial \xi}(\mu^2 u_\xi) = u_{\tau\tau} \quad (4.3)$$

or

$$u_{\tau\tau} - \mu^2 u_{\xi\xi} = 0 \quad (4.4)$$

Also the derivative of third equation in (4.1) can be expressed as

$$\begin{aligned} \mathcal{M}_{\xi\xi} &= \nu_\xi \alpha - \lambda \alpha \theta_\xi - \gamma^2 \theta_{\tau\tau\xi} \\ &= v_{\tau\tau} \alpha - \lambda \alpha \left(\frac{1}{\alpha} v_{\xi\xi}\right) - \gamma^2 \left(\frac{1}{\alpha}\right) v_{\xi\xi\tau\tau} \end{aligned} \quad (4.5)$$

or

$$\frac{\partial^2}{\partial \xi^2} \left(-\frac{1}{\alpha} v_{\xi\xi}\right) = v_{\tau\tau} \alpha - \lambda \alpha \left(\frac{1}{\alpha} v_{\xi\xi}\right) - \gamma^2 \left(\frac{1}{\alpha}\right) v_{\xi\xi\tau\tau} \quad (4.6)$$

which can be re-written as

$$v_{\xi\xi\xi\xi} + v_{\tau\tau} \alpha^2 - \lambda \alpha v_{\xi\xi} - \gamma^2 v_{\xi\xi\tau\tau} = 0 \quad (4.7)$$

In summary, for small displacements, the differential equations describing the axial and transversal vibration are

$$\begin{aligned} u_{\tau\tau} - \mu^2 u_{\xi\xi} &= 0, \\ v_{\xi\xi\xi\xi} + v_{\tau\tau} \alpha^2 - \lambda \alpha v_{\xi\xi} - \gamma^2 v_{\xi\xi\tau\tau} &= 0 \end{aligned} \quad (4.8)$$

From the boundary conditions, Eqs. (2.54) one obtains

$$\begin{aligned} u(\tau, \xi = 0) &= 0, & u_\xi(\tau, \xi = 1) &= 0, \\ v(\tau, \xi = 0) &= 0, & v(\tau, \xi = 1) &= 0, & v_{\xi\xi}(\tau, \xi = 0) &= 0, & v_{\xi\xi}(\tau, \xi = 1) &= 0 \end{aligned} \quad (4.9)$$

As can be observed from Eqs.(4.8), the two differential equations are decoupled. The solution of system (4.8), (4.9) is assumed in the form

$$\begin{aligned} u(\xi, \tau) &= U(\xi) \sin(\omega_1 \tau + \phi_1), \\ v(\xi, \tau) &= V(\xi) \sin(\omega_2 \tau + \phi_2) \end{aligned} \quad (4.10)$$

Where ω_1 and ω_2 are the frequencies of axial and transversal vibrations and ϕ_1 and ϕ_2 are constants. Substituting Eqs. (4.10) into Eqs. (4.8) yields

$$\begin{aligned} U_{\xi\xi}(\xi) + \left[\frac{\omega_1}{\mu}\right]^2 U(\xi) &= 0, \\ V_{\xi\xi\xi\xi}(\xi) + ([\omega_2 \gamma]^2 - \lambda \alpha) V_{\xi\xi}(\xi) - [\omega_2 \alpha]^2 V(\xi) &= 0 \end{aligned} \quad (4.11)$$

Considering the boundary conditions, Eqs. (4.9), the solution of the above equations can be obtained as [5]

$$\begin{aligned} U_n(\xi) &= C_{1n} \sin \left[\frac{2n-1}{2} \pi \xi \right], \\ V_n(\xi) &= C_{2n} \sin [n\pi\xi], \quad n = 1, 2, 3, \dots \end{aligned} \quad (4.12)$$

where C_{1n} and C_{2n} are constants. Here $U_n(\xi)$ and $V_n(\xi)$ are the mode shapes for the axial and transversal vibration of the beam respectively. For $n = 1$ the corresponding frequencies are [5]

$$\begin{aligned} \omega_1 &= \frac{\mu\pi}{2}, \\ \omega_2 &= \sqrt{\pi^2 \frac{\pi^2 - \alpha\lambda}{\alpha^2 + \gamma^2\pi^2}} \end{aligned} \quad (4.13)$$

which are the natural frequencies for the first mode axial and transversal vibration of a 2D extensible elastic beam.

4.2 Nonlinear Equations

The next step is to find a solution for the non-linear equations of a 2D extensible beam, i.e. Eqs. (2.53) and (2.54), which are nonlinear PDEs in space and time. These PDEs and associated boundary conditions form an initial boundary-value problem. In general, the exact or closed-form solutions for this class of problems are not known. Consequently, one seeks approximate solutions of the original problem. This requires firstly approximating the non-linear terms by Taylor series expansion and secondly converting the PDEs into more manageable low-order sets of ODEs. The nonlinearities in the beam equations are in terms of sinusoidal functions.

The effect of including higher order Taylor series terms on the maximum deflection of the static beam are investigated and results are shown in Figs. (4.1) and (4.2). In Fig. (4.1) for $\lambda = 1.5\lambda_{cr}$ and different μ , the maximum deflection of the beam in static case obtained from the exact solution and Taylor series expansions are compared. In Fig. (4.2) for $\mu = 10$ and different λ results are compared. These figures show that as μ increases, an error of Taylor series expansion decreases. Furthermore for a larger λ one gets larger errors by using Taylor series expansion. Accordingly, for the range of μ and λ ($\mu < 1000, \lambda < 1.1\lambda_{cr}$), using 5th order Taylor series expansion should guarantee the error of static deflection to be less than 0.01%. Henceforth I use 5th order Taylor series expansion in approximations.

4.2.1 Galerkin Method

There are two classes of approximate solutions of initial boundary-value problems: numerical methods and analytical methods. Numerical methods (e.g., finite differences, finite elements, and boundary elements) replace the initial boundary-value problem by a set of nonlinear algebraic equations, which are solved by using a variety

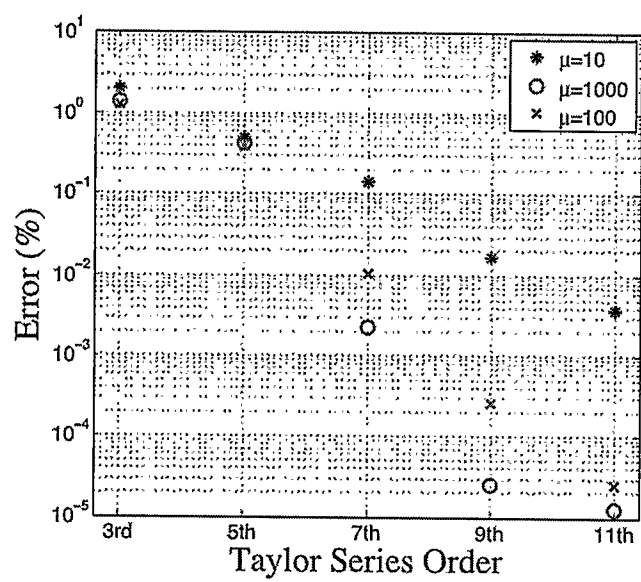


Figure 4.1: The error in calculation of maximum deflection (between Taylor series approximation and exact non-linear terms), $\lambda = 1.5\lambda_{cr}$

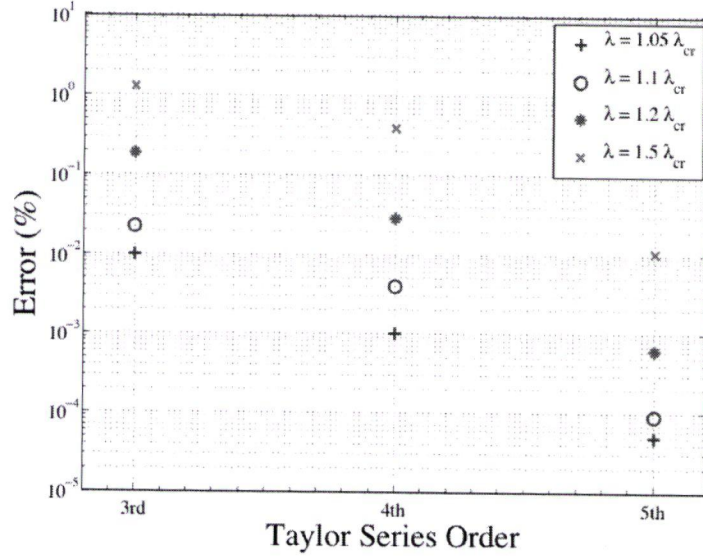


Figure 4.2: The error in calculation of maximum deflection (between Taylor series approximation and exact non-linear terms), $\mu = 10$

of techniques. Analytical methods can be divided into two categories: direct and discretization techniques. For weakly nonlinear systems, direct techniques, such as perturbation methods, are used to solve the nonlinear partial differential equations with associated boundary conditions. If, for example, $q(x, t)$ denote the dependent variable of a PDE, in discretization method, one assumes the solution in the form [7]

$$q(x, t) = \sum_{n=1}^N \phi_n(x) y_n(t) \quad (4.14)$$

where N is an integer. Then, one either assumes the temporal functions $y_n(t)$ time discretization, or the spatial functions $\phi_n(x)$ space discretization. With time discretization, the $y_n(t)$ are usually taken to be harmonic and the method is called the method of harmonic balance. The result is a set of nonlinearly coupled ODEs, in space, for the $\phi_n(x)$. With space discretization, the $\phi_n(x)$ are assumed and used

in a variational or weighted-residual method. The result is a set of nonlinear coupled ODEs, in time, for the $y_n(t)$. In the method of weighted residuals (e.g., Galerkin, collocation, least squares) one works directly with the differential equations and associated boundary conditions. In the variational methods (e.g., Rayleigh-Ritz), one uses a functional related to the differential equations and associated boundary conditions and works with the problem in a weak form. The functional is defined as an operator that maps a function into a scalar or a functional is a function of functions, such as the integration operator. Variational methods are not applicable to all problems and thus lack generality [7].

4.2.2 Case I: First Mode Shape Expansion

For our specific problem I use the Galerkin discretization method. The vibrational mode shapes are considered as known spatial functions (mode shape expansion) and I obtain a set of ODEs for the temporal functions, $y_n(t)$. The vibrational mode shapes for a 2D extensible beam are expressed in Eqs. (4.12). Using these mode shapes, one can assume

$$\begin{aligned}
 \mathcal{H}(\xi, \tau) &= \sum_{n=1}^N \mathcal{H}_n(\tau) \cos \left[\frac{2n-1}{2} \pi \xi \right], & \mathcal{V}(\xi, \tau) &= \sum_{n=1}^N \mathcal{V}_n(\tau) \cos [n\pi\xi], \\
 \mathcal{M}(\xi, \tau) &= \sum_{n=1}^N \mathcal{M}_n(\tau) \sin [n\pi\xi], & u(\xi, \tau) &= \sum_{n=1}^N u_n(\tau) \sin \left[\frac{2n-1}{2} \pi \xi \right], \\
 v(\xi, \tau) &= \sum_{n=1}^N v_n(\tau) \sin [n\pi\xi], & \theta(\xi, \tau) &= \sum_{n=1}^N \theta_n(\tau) \cos [n\pi\xi]
 \end{aligned} \tag{4.15}$$

The first approximation to the solution of nonlinear equations is to set $N = 1$ in the above equations, i.e. using only the first mode shape expansion. By expanding the nonlinear terms into 5th order of Taylor series and substituting Eqs. (4.15) into

(2.53), integrating the equations over the length of the beam and for the first mode shape expansion, one obtains

$$\begin{aligned}
\mathcal{H}_1(\tau) &= -\frac{2}{\pi}u_{1,\tau\tau}(\tau), \\
\mathcal{V}_1(\tau) &= -\frac{1}{\pi}v_{1,\tau\tau}(\tau) - \frac{1}{2}f_1(\tau) - \frac{1}{\pi}Cv_{1,\tau}(\tau), \\
\mathcal{M}_1(\tau) &= \frac{1}{\pi}u_1(\tau)\mathcal{V}_1(\tau) + \frac{1}{\pi}\mathcal{V}_1(\tau)\alpha + \lambda v_1(\tau) - \frac{2}{\pi}\mathcal{H}_1(\tau)v_1(\tau) - \frac{1}{\pi}\gamma^2\theta_{1,\tau\tau}(\tau), \\
u_1(\tau) &= -\frac{1}{4}\theta_1^2(\tau) \left[1 - \frac{1}{16}\theta_1^2(\tau)\right] + \frac{\lambda}{2\mu^2}\theta_1^2(\tau) \left[1 - \frac{1}{4}\theta_1^2(\tau)\right] \\
&\quad + \frac{2}{\pi\mu^2}\mathcal{H}_1(\tau) \left[1 - \frac{7}{15}\theta_1^2(\tau) + \frac{107}{945}\theta_1^4(\tau)\right] \\
&\quad + \frac{1}{2\mu^2}\mathcal{V}_1(\tau)\theta_1(\tau) \left[1 - \frac{1}{2}\theta_1^2(\tau) + \frac{1}{12}\theta_1^4(\tau)\right], \\
v_1(\tau) &= \frac{1}{\pi}\theta_1(\tau) \left[\alpha \left(1 + \frac{1}{6}\theta_1^2(\tau) + \frac{1}{20}\theta_1^4(\tau)\right) + u_1(\tau) \left(1 + \frac{7}{45}\theta_1^2(\tau) + \frac{214}{4725}\theta_1^4(\tau)\right)\right], \\
\theta_1(\tau) &= \frac{1}{\pi}\mathcal{M}_1(\tau)
\end{aligned} \tag{4.16}$$

where $f_1(\tau) = -\mathcal{A} \cos(\Omega\tau)$ is the excitation force. In simplified form, Eqs. (4.16) can be expressed as

$$\begin{aligned}
A_1\theta_{1,\tau\tau}(\tau) + B_1u_{1,\tau\tau}(\tau) &= E_1, \\
A_2\theta_{1,\tau\tau}(\tau) + B_2u_{1,\tau\tau}(\tau) &= E_2
\end{aligned} \tag{4.17}$$

where

$$\begin{aligned}
A_1 &= \frac{1}{\pi^2} \bar{\alpha} \bar{Q} + \frac{1}{\pi} \gamma^2, \\
B_1 &= \frac{1}{\pi^2} \bar{L} - \frac{4}{\pi^2} v_1(\tau), \\
E_1 &= \lambda v_1(\tau) - \pi \theta_1(\tau) - \frac{1}{\pi^2} \bar{\alpha} \bar{M} - \frac{1}{2\pi} f_1(\tau) \bar{\alpha} - \frac{1}{\pi^2} C [\bar{L} u_{1,\tau}(\tau) + \bar{Q} \theta_{1,\tau}(\tau)] \bar{\alpha}, \\
A_2 &= \frac{1}{2\mu^2 \pi} \bar{Q} \theta_1(\tau) \left(1 - \frac{1}{2} \theta_1^2(\tau) \right), \\
B_2 &= \frac{1}{2\mu^2 \pi} \bar{L} \theta_1(\tau) \left(1 - \frac{1}{2} \theta_1^2(\tau) \right) + \frac{4}{\pi^2 \mu^2} \left(1 - \frac{7}{15} \theta_1^2(\tau) \right), \\
E_2 &= -u_1(\tau) - \frac{1}{4} \theta_1^2(\tau) + \frac{\lambda}{2\mu^2} \theta_1^2(\tau) - \frac{1}{2\mu^2 \pi} \bar{M} \theta_1(\tau) - \frac{1}{4\mu^2} f_1(\tau) \theta_1(\tau) \left(1 - \frac{1}{2} \theta_1^2(\tau) \right) \\
&\quad - \frac{1}{2\pi \mu^2} C \theta_1(\tau) \left(1 - \frac{1}{2} \theta_1^2(\tau) \right) [\bar{L} u_{1,\tau}(\tau) + \bar{Q} \theta_{1,\tau}(\tau)]
\end{aligned} \tag{4.18}$$

In the above equations

$$\bar{\alpha} = \alpha + u_1(\tau) \tag{4.19}$$

where α is defined in Eq. (4.2). Also in Eqs.(4.17), $v_1(\tau)$ is given by the fifth equation in (4.16). I have defined $v_{1,\tau}(\tau) = \bar{Q} \theta_{1,\tau}(\tau) + \bar{L} u_{1,\tau}(\tau)$ and $v_{1,\tau\tau}(\tau) = \bar{Q} \theta_{1,\tau\tau}(\tau) + \bar{L} u_{1,\tau\tau}(\tau) + \bar{M}$, where

$$\begin{aligned}
\bar{Q} &= \frac{1}{\pi} \left[\alpha \left(1 + \frac{1}{2} \theta_1^2(\tau) + \frac{1}{4} \theta_1^4(\tau) \right) + u_1(\tau) \left(1 + \frac{7}{15} \theta_1^2(\tau) + \frac{214}{945} \theta_1^4(\tau) \right) \right], \\
\bar{L} &= \frac{1}{\pi} \theta_1(\tau) \left[1 + \frac{7}{45} \theta_1^2(\tau) + \frac{214}{4725} \theta_1^4(\tau) \right], \\
\bar{M} &= \frac{1}{\pi} \theta_1(\tau) \theta_{1,\tau}^2(\tau) \alpha [1 + \theta_1^2(\tau)] + \frac{1}{\pi} u_{1,\tau}(\tau) \theta_{1,\tau}(\tau) \theta_1^2(\tau) \left[\frac{14}{15} + \frac{428}{945} \theta_1^2(\tau) \right] \\
&\quad + \frac{2}{\pi} u_{1,\tau}(\tau) \theta_{1,\tau}(\tau) + \frac{14}{15} u_1(\tau) \theta_1(\tau) \theta_{1,\tau}^2(\tau)
\end{aligned} \tag{4.20}$$

As can be seen from Eqs. (4.17), the final approximated equations are two second order ODEs. These equations have been obtained by employing the Taylor series

expansion and the first mode shape expansion. In general, by considering N number of the mode shapes, one gets the final ODEs in the form of

$$\mathcal{R}\mathbf{V}_{\tau\tau} = \mathbf{E} \quad (4.21)$$

where \mathcal{R} is a $2N \times 2N$ matrix of coefficients, \mathbf{E} is a $2N$ column vector and

$$\mathbf{V} = \{\theta_1(\tau) \ \theta_2(\tau) \ \dots \ \theta_N(\tau) \ u_1(\tau) \ u_2(\tau) \ \dots \ u_N(\tau)\}^T \quad (4.22)$$

For $N = 1$, the equations are in the form of Eqs. (4.17). Here I derive the equations for the $N = 2$ case as well and in the next section I study the effect of including higher order modes in Galerkin mode shape expansion method.

4.2.3 Case II: First & Second Mode Shape Expansion

By expanding the nonlinear terms into 5th order of Taylor series and substituting Eqs. (4.15), ($N = 2$), into (2.53), integrating the equations over the length of the beam

for the undamped case one obtains

$$\begin{aligned}\mathcal{H}_1(\tau) &= -\frac{2}{\pi}u_{1,\tau\tau}(\tau), \\ \mathcal{H}_2(\tau) &= -\frac{2}{3\pi}u_{2,\tau\tau}(\tau),\end{aligned}$$

$$\begin{aligned}\mathcal{V}_1(\tau) &= -\frac{1}{\pi}v_{1,\tau\tau}(\tau) - \frac{4}{\pi^2}f_1(\tau), \\ \mathcal{V}_2(\tau) &= -\frac{1}{2\pi}v_{2,\tau\tau}(\tau),\end{aligned}$$

$$\begin{aligned}\mathcal{M}_1(\tau) &= \frac{11}{35}u_1(\tau)\mathcal{V}_1(\tau) + \frac{1}{\pi}\alpha\mathcal{V}_1(\tau) + \lambda v_1(\tau) - \frac{22}{35}\mathcal{H}_1(\tau)v_1(\tau) \\ &\quad - \frac{\gamma^2}{\pi}\theta_{1,\tau\tau}(\tau) + \frac{2}{15}\mathcal{H}_2(\tau)v_1(\tau) - \frac{4}{21}\mathcal{H}_1(\tau)v_2(\tau) - \frac{12}{55}\mathcal{H}_2(\tau)v_2(\tau) \\ &\quad - \frac{1}{5}u_2(\tau)\mathcal{V}_1(\tau) + \frac{1}{21}u_1(\tau)\mathcal{V}_2(\tau) + \frac{9}{55}u_2(\tau)\mathcal{V}_2(\tau), \\ \mathcal{M}_2(\tau) &= -\frac{7}{10}u_2(\tau)\mathcal{V}_2(\tau) + \frac{1}{2\pi}\alpha\mathcal{V}_2 + \lambda v_2(\tau) + \frac{14}{15}\mathcal{H}_2(\tau)v_2(\tau) \\ &\quad - \frac{\gamma^2}{2\pi}\theta_{2,\tau\tau}(\tau) + \frac{1}{5}\mathcal{H}_1(\tau)v_1(\tau) - \frac{26}{35}\mathcal{H}_1(\tau)v_2(\tau) + \frac{3}{7}\mathcal{H}_2(\tau)v_1(\tau) \\ &\quad - \frac{9}{14}u_2(\tau)\mathcal{V}_1(\tau) + \frac{13}{70}u_1(\tau)\mathcal{V}_2(\tau) + \frac{1}{10}u_1(\tau)\mathcal{V}_1(\tau),\end{aligned}$$

$$\begin{aligned}u_1(\tau) &= -\frac{28}{15\pi^2}\theta_1^2(\tau) \left[1 - \frac{2\lambda}{\mu^2} \left(1 + \frac{107}{294}\theta_1^2(\tau) \right) \right] \\ &\quad + \frac{2}{\pi\mu^2}\mathcal{H}_1(\tau) \left[1 - \frac{1}{2}(\theta_1^2(\tau) + \theta_2^2(\tau)) + \frac{3}{32}(\theta_1^4(\tau) + \theta_2^4(\tau)) \right] \\ &\quad + \frac{56}{15\pi^2\mu^2} \left[1 - \frac{214}{441}\theta_1^2(\tau) \right] \\ &\quad - \frac{124}{63\pi^2}\theta_2^2(\tau) \left(1 - \frac{2\lambda}{\mu^2} \right) + \frac{1}{\pi^2\mu^2}\theta_2(\tau) \left(\frac{152}{105}\mathcal{V}_1(\tau) + \frac{248}{63}\mathcal{V}_2(\tau) \right) \\ &\quad + \theta_1(\tau)\theta_2(\tau) \left\{ -\frac{152}{105\pi^2} \left(1 - \frac{2\lambda}{\mu^2} \right) - \frac{1}{\pi\mu^2}\mathcal{H}_1(\tau) \left(1 - \frac{1}{2}\theta_1^2(\tau) - \frac{3}{4}\theta_1(\tau)\theta_2(\tau) \right. \right. \\ &\quad \left. \left. - \frac{3}{8}\theta_2^2(\tau) \right) - \frac{1}{\pi\mu^2}\mathcal{H}_2(\tau) \left(1 - \frac{1}{2}\theta_1^2(\tau) - \frac{3}{8}\theta_2^2(\tau) - \frac{9}{16}\theta_1(\tau)\theta_2(\tau) \right) \right\} \\ &\quad + \frac{152}{105\pi^2\mu^2}\mathcal{V}_2(\tau)\theta_1(\tau) - \frac{1}{2\pi\mu^2}\theta_1^2(\tau)\mathcal{H}_2(\tau) \left(1 - \frac{1}{4}\theta_1^2(\tau) \right),\end{aligned}$$

$$\begin{aligned}
u_2(\tau) = & -\frac{4}{63\pi^2}\theta_1^2(\tau)\left(1-\frac{2\lambda}{\mu^2}\right) + \frac{2}{3\mu^2\pi}\mathcal{H}_2(\tau)\left(1-\frac{1}{2}(\theta_1^2(\tau)+\theta_2^2(\tau))\right) \\
& + \frac{8}{63\pi^2\mu^2}\mathcal{V}_1(\tau)\theta_1(\tau) + \frac{92}{495\pi^2}\theta_2^2(\tau)\left(1-\frac{2\lambda}{\mu^2}\right) \\
& + \frac{88}{135\pi^2\mu^2}(\mathcal{V}_2(\tau)\theta_1(\tau)+\mathcal{V}_1(\tau)\theta_2(\tau)) - \frac{184}{495\pi^2\mu^2}\mathcal{V}_2(\tau)\theta_2(\tau) \\
& + \frac{1}{\pi^2}\theta_1(\tau)\theta_2(\tau)\left\{-\frac{88}{135}\left(1-\frac{2\lambda}{\mu^2}\right)\right. \\
& - \frac{1}{3\pi\mu^2}\mathcal{H}_1(\tau)\left(1-\frac{1}{2}\theta_1^2(\tau)-\frac{3}{8}\theta_2^2(\tau)-\frac{9}{16}\theta_1(\tau)\theta_2(\tau)\right) \\
& \left.- \frac{1}{3\pi\mu^2}\mathcal{H}_2(\tau)\left(1-\frac{3}{8}(\theta_1^2(\tau)+\theta_2^2(\tau))-\frac{3}{4}\theta_1(\tau)\theta_2(\tau)-\frac{260}{693}\frac{\lambda}{\pi^2\mu^2}\theta_1(\tau)\theta_2(\tau)\right)\right\} \\
& + \frac{1}{16\pi\mu^2}\mathcal{H}_2(\tau)(\theta_1^4(\tau)+\theta_2^4(\tau)) - \frac{1}{6\pi\mu^2}\mathcal{H}_1(\tau)\theta_1^2(\tau)\left(1-\frac{1}{4}\theta_1^2(\tau)\right),
\end{aligned}$$

$$\begin{aligned}
v_1(\tau) = & \theta_1(\tau)\left\{\frac{1}{\pi}\alpha\left(1+\frac{1}{5}\theta_1^2(\tau)+\frac{11}{35}\theta_2^2(\tau)\right)\right. \\
& + u_1(\tau)\left(\frac{11}{35}+\frac{211}{3465}\theta_1^2(\tau)\right) - \frac{1}{5}u_2(\tau)\left(1+\frac{1}{91}\theta_1^2(\tau)\right)\left.\right\} \\
& + \theta_2(\tau)\left(\frac{1}{21}u_1(\tau)+\frac{9}{55}u_2(\tau)\right) + \frac{103}{385}u_2(\tau)\theta_1^2(\tau)\theta_2(\tau), \\
v_2(\tau) = & \theta_2(\tau)\left\{\frac{1}{2\pi}\alpha\left(1-\frac{1}{5}\theta_1^2(\tau)+\frac{9}{35}\theta_2^2(\tau)\right) + u_2(\tau)\left(\frac{7}{10}-\frac{17}{182}\theta_1^2(\tau)\right)\right. \\
& + \frac{13}{70}u_1(\tau)\left.\right\} + \theta_1(\tau)\left(-\frac{1}{10}u_1(\tau)-\frac{9}{14}u_2(\tau)\right) \\
& + \theta_1^3(\tau)\left(-\frac{13}{630}u_1(\tau)-\frac{93}{770}u_2(\tau)\right) - \frac{13}{70}u_2(\tau)\theta_1(\tau)\theta_2^2(\tau),
\end{aligned}$$

$$\theta_1(\tau) = \frac{1}{\pi}\mathcal{M}_1(\tau),$$

$$\theta_2(\tau) = \frac{1}{2\pi}\mathcal{M}_2(\tau)$$

(4.23)

In simplified form, Eqs. (4.23) can be expressed in the form of Eq. (4.21) with

$$\mathcal{R} = \begin{bmatrix} A_1 & B_1 & C_1 & D_1 \\ A_2 & B_2 & C_2 & D_2 \\ A_3 & B_3 & C_3 & D_3 \\ A_4 & B_4 & C_4 & D_4 \end{bmatrix}$$

$$\mathbf{E} = \{E_1 \ E_2 \ E_3 \ E_4\}^T$$

$$\mathbf{V} = \{\theta_1(\tau) \ \theta_2(\tau) \ u_1(\tau) \ u_2(\tau)\}^T \quad (4.24)$$

where

$$\begin{aligned} A_1 &= \frac{1}{\pi} [\bar{Q}_{11}\Delta_1 + \bar{Q}_{21}\Gamma_1], \\ B_1 &= \frac{1}{\pi} [\bar{Q}_{12}\Delta_1 + \bar{Q}_{22}\Gamma_1] - \frac{2}{3} \frac{\gamma^2}{\pi}, \\ C_1 &= \frac{1}{\pi} [\bar{L}_{11}\Delta_1 + \bar{L}_{21}\Gamma_1] - \frac{8}{15\pi} v_1(\tau) + \frac{208}{105\pi} v_2(\tau), \\ D_1 &= \frac{1}{\pi} [\bar{L}_{12}\Delta_1 + \bar{L}_{22}\Gamma_1] - \frac{8}{21\pi} v_1(\tau) - \frac{112}{135\pi} v_2(\tau), \\ E_1 &= -\left[\frac{1}{\pi} (\bar{R}_1\Delta_1 + \bar{R}_2\Gamma_1) + \frac{4}{3} \lambda v_2(\tau) \right. \\ &\quad \left. - \frac{8}{3} \pi \theta_2(\tau) + \frac{1}{\pi^2} f_1(\tau) \left(\frac{8}{15} u_1(\tau) + \frac{24}{7} u_2(\tau) \right) \right], \end{aligned}$$

$$\begin{aligned} A_2 &= \frac{1}{\pi} [\bar{Q}_{11}\Delta_2 + \bar{Q}_{21}\Gamma_2] + \frac{4}{3} \frac{\gamma^2}{\pi}, \\ B_2 &= \frac{1}{\pi} [\bar{Q}_{12}\Delta_2 + \bar{Q}_{22}\Gamma_2], \\ C_2 &= \frac{1}{\pi} [\bar{L}_{11}\Delta_2 + \bar{L}_{21}\Gamma_2] - \frac{176}{105\pi} v_1(\tau) - \frac{32}{63\pi} v_2(\tau), \\ D_2 &= \frac{1}{\pi} [\bar{L}_{12}\Delta_2 + \bar{L}_{22}\Gamma_2] + \frac{16}{135\pi} v_1(\tau) - \frac{32}{165} v_2(\tau), \\ E_2 &= -\left[\frac{1}{\pi} (\bar{R}_1\Delta_2 + \bar{R}_2\Gamma_2) - \frac{4}{3} \lambda v_1(\tau) + \frac{4}{3} \pi \theta_1(\tau) \right. \\ &\quad \left. + f_1(\tau) \left(\frac{16}{3\pi^3} \alpha + \frac{176}{105\pi^2} u_1(\tau) - \frac{16}{15\pi^2} u_2(\tau) \right) \right], \end{aligned}$$

$$\begin{aligned}
A_3 &= \frac{1}{\pi^3 \mu^2} [\bar{Q}_{11} \Delta_3 + \bar{Q}_{21} \Gamma_3], \\
B_3 &= \frac{1}{\pi^3 \mu^2} [\bar{Q}_{12} \Delta_3 + \bar{Q}_{22} \Gamma_3], \\
C_3 &= \frac{1}{\pi^3 \mu^2} [\bar{L}_{11} \Delta_3 + \bar{L}_{21} \Gamma_3] + \frac{4}{\pi^2 \mu^2} \left(1 + \frac{1}{2} (\theta_1^2(\tau) + \theta_2^2(\tau)) - \frac{3}{32} (\theta_1^4(\tau) + \theta_2^4(\tau)) \right) \\
&\quad + \frac{2}{\pi^2 \mu^2} \theta_1(\tau) \theta_2(\tau) \left(1 - \frac{1}{2} \theta_1^2(\tau) - \frac{3}{8} \theta_2^2(\tau) - \frac{3}{4} \theta_1(\tau) \theta_2(\tau) \right), \\
D_3 &= \frac{1}{\pi^3 \mu^2} [\bar{L}_{12} \Delta_3 + \bar{L}_{22} \Gamma_3] + \frac{1}{3\pi^2 \mu^2} \theta_1^2(\tau) \left(1 - \frac{1}{4} \theta_1^2(\tau) \right) \\
&\quad + \frac{2}{3\pi^2 \mu^2} \theta_1(\tau) \theta_2(\tau) \left(1 - \frac{1}{2} \theta_1^2(\tau) - \frac{3}{8} \theta_2^2(\tau) - \frac{9}{16} \theta_1(\tau) \theta_2(\tau) \right), \\
E_3 &= -\left[\frac{1}{\pi^3 \mu^2} (\bar{R}_1 \Delta_3 + \bar{R}_2 \Gamma_3) + u_1(\tau) - \frac{28}{15\pi^2} \left(1 - \frac{2\lambda}{\mu^2} \right) \theta_1^2(\tau) \right. \\
&\quad - \frac{214}{315} \frac{\lambda}{\pi^2 \mu^2} \theta_1^4(\tau) - \frac{152}{105\pi^2} \theta_1(\tau) \theta_2(\tau) \left(1 - \frac{2\lambda}{\mu^2} \right) \\
&\quad \left. - \frac{124}{63\pi^2} \theta_2^2(\tau) \left(1 - \frac{2\lambda}{\mu^2} \right) + \frac{1}{\pi^4 \mu^2} f_1(\tau) \left(-\frac{224}{15} \theta_1(\tau) + \frac{6848}{945} \theta_1^3(\tau) - \frac{608}{105} \theta_2(\tau) \right) \right]
\end{aligned}$$

$$\begin{aligned}
A_4 &= \frac{1}{\pi^3 \mu^2} [\bar{Q}_{11} \Delta_4 + \bar{Q}_{21} \Gamma_4], \\
B_4 &= \frac{1}{\pi^3 \mu^2} [\bar{Q}_{12} \Delta_4 + \bar{Q}_{22} \Gamma_4], \\
C_4 &= \frac{1}{\pi^3 \mu^2} [\bar{L}_{11} \Delta_4 + \bar{L}_{21} \Gamma_4] + \frac{1}{3\pi^2 \mu^2} \theta_1^2(\tau) \left(1 - \frac{1}{4} \theta_1^2(\tau) \right) \\
&\quad + \frac{2}{3\pi^2 \mu^2} \theta_1(\tau) \theta_2(\tau) \left(1 - \frac{1}{2} \theta_1^2(\tau) - \frac{3}{8} \theta_2^2(\tau) - \frac{9}{16} \theta_1(\tau) \theta_2(\tau) \right), \\
D_4 &= \frac{1}{\pi^3 \mu^2} [\bar{L}_{12} \Delta_4 + \bar{L}_{22} \Gamma_4] + \frac{4}{9\pi^2 \mu^2} \left(1 + \frac{1}{2} (\theta_1^2(\tau) + \theta_2^2(\tau)) - \frac{3}{32} (\theta_1^4(\tau) + \theta_2^4(\tau)) \right) \\
&\quad + \frac{2}{9\pi^2 \mu^2} \theta_1(\tau) \theta_2(\tau) \left(1 - \frac{3}{8} (\theta_1^2(\tau) + \theta_2^2(\tau)) - \frac{3}{4} \theta_1(\tau) \theta_2(\tau) \right),
\end{aligned}$$

$$\begin{aligned}
E_4 = & -\left[\frac{1}{\pi^3 \mu^2} (\bar{R}_1 \Delta_4 + \bar{R}_2 \Gamma_4) - u_2(\tau) - \frac{4}{63\pi^2} \left(1 - \frac{2\lambda}{\mu^2} \right) \theta_1^2(\tau) \right. \\
& - \frac{88}{135\pi^2} \theta_1(\tau) \theta_2(\tau) \left(1 - \frac{2\lambda}{\mu^2} \right) + \frac{92}{495\pi^2} \theta_2^2(\tau) \left(1 - \frac{2\lambda}{\mu^2} \right) - \frac{260}{693} \frac{\lambda}{\pi^2 \mu^2} \theta_1^2(\tau) \theta_2^2(\tau) \\
& \left. + \frac{1}{\pi^4 \mu^2} f_1(\tau) \left(-\frac{32}{63} \theta_1(\tau) - \frac{352}{135} \theta_2(\tau) \right) \right]
\end{aligned} \tag{4.25}$$

I have defined $v_{1,\tau\tau}(\tau) = \bar{Q}_{11}\theta_{1,\tau\tau}(\tau) + \bar{Q}_{12}\theta_{2,\tau\tau}(\tau) + \bar{L}_{11}u_{1,\tau\tau}(\tau) + \bar{L}_{12}u_{2,\tau\tau}(\tau) + \bar{R}_1$ and $v_{2,\tau\tau}(\tau) = \bar{Q}_{21}\theta_{1,\tau\tau}(\tau) + \bar{Q}_{22}\theta_{2,\tau\tau}(\tau) + \bar{L}_{21}u_{1,\tau\tau}(\tau) + \bar{L}_{22}u_{2,\tau\tau}(\tau) + \bar{R}_2$, where

$$\begin{aligned}
\bar{Q}_{11} = & \frac{1}{\pi} \alpha \left[1 + \frac{3}{5} \theta_1^2(\tau) + \frac{11}{35} \theta_2^2(\tau) \right] + u_1(\tau) \left(\frac{11}{35} + \frac{211}{1155} \theta_1^2(\tau) \right) \\
& - \frac{1}{5} u_2(\tau) \left(1 - \frac{3}{91} \theta_1^2(\tau) \right) + \frac{206}{385} u_2(\tau) \theta_1(\tau) \theta_2(\tau), \\
\bar{Q}_{12} = & \frac{22}{35\pi} \theta_1(\tau) \theta_2(\tau) \alpha + \frac{1}{21} u_1(\tau) + \frac{9}{55} u_2(\tau) + \frac{103}{385} u_2(\tau) \theta_1^2(\tau), \\
\bar{L}_{11} = & \theta_1(\tau) \left[\frac{11}{35} + \frac{211}{3465} \theta_1^2(\tau) \right] + \frac{1}{21} \theta_2(\tau), \\
\bar{L}_{12} = & -\frac{1}{5} \theta_1(\tau) \left[1 + \frac{1}{91} \theta_1^2(\tau) \right] + \frac{9}{55} \theta_2(\tau) + \frac{103}{385} \theta_1^2(\tau) \theta_2(\tau), \\
\bar{R}_1 = & \frac{22}{35} u_{1,\tau}(\tau) \theta_{1,\tau}(\tau) + \frac{422}{1155} \theta_1^2(\tau) u_{1,\tau}(\tau) \theta_{1,\tau}(\tau) - \frac{2}{5} u_{2,\tau}(\tau) \theta_{1,\tau}(\tau) \\
& - \frac{6}{455} \theta_1^2(\tau) u_{2,\tau}(\tau) \theta_{1,\tau}(\tau) + \frac{412}{385} \theta_1(\tau) \theta_2(\tau) u_{2,\tau}(\tau) \theta_{1,\tau}(\tau) + \frac{6}{5\pi} \theta_1(\tau) \theta_{1,\tau}^2(\tau) \alpha \\
& + \frac{422}{1155} u_1(\tau) \theta_1(\tau) \theta_{1,\tau}^2(\tau) - \frac{6}{455} u_2(\tau) \theta_1(\tau) \theta_{1,\tau}^2(\tau) + \frac{206}{385} u_2(\tau) \theta_2(\tau) \theta_{1,\tau}^2(\tau) \\
& + \frac{2}{21} u_{1,\tau}(\tau) \theta_{2,\tau}(\tau) + \frac{18}{55} u_{2,\tau}(\tau) \theta_{2,\tau}(\tau) + \frac{206}{385} \theta_1^2(\tau) u_{2,\tau}(\tau) \theta_{2,\tau}^2(\tau) \\
& + \frac{412}{385} u_2(\tau) \theta_1(\tau) \theta_{1,\tau}(\tau) \theta_{2,\tau}(\tau) + \frac{44}{35\pi} \alpha \theta_2(\tau) \theta_{1,\tau}(\tau) \theta_{2,\tau}(\tau) + \frac{22}{35\pi} \alpha \theta_1(\tau) \theta_{2,\tau}^2(\tau),
\end{aligned}$$

$$\begin{aligned}
\bar{Q}_{21} &= -\frac{\alpha}{5\pi}\theta_1(\tau)\theta_2(\tau) - \frac{1}{10}u_1(\tau) \left(1 + \frac{13}{21}\theta_1^2(\tau)\right) \\
&\quad + u_2(\tau) \left(-\frac{9}{14} - \frac{279}{770}\theta_1^2(\tau) - \frac{17}{91}\theta_1(\tau)\theta_2(\tau) - \frac{13}{70}\theta_2^2(\tau)\right), \\
\bar{Q}_{22} &= \frac{\alpha}{2\pi} \left(1 - \frac{1}{5}\theta_1^2(\tau) + \frac{27}{35}\theta_2^2(\tau)\right) + \frac{13}{70}u_1(\tau) \\
&\quad + u_2(\tau) \left(\frac{7}{10} - \frac{17}{182}\theta_1^2(\tau) - \frac{13}{35}\theta_1(\tau)\theta_2(\tau)\right), \\
\bar{L}_{21} &= \frac{1}{10}\theta_1(\tau) \left(1 - \frac{13}{63}\theta_1^2(\tau) + \frac{13}{70}\theta_2(\tau)\right), \\
\bar{L}_{22} &= -\theta_1(\tau) \left(\frac{19}{14} + \frac{93}{770}\theta_1^2(\tau)\right) - \frac{7}{10}\theta_2(\tau) - \theta_1(\tau)\theta_2(\tau) \left(\frac{17}{182}\theta_1(\tau) + \frac{13}{70}\theta_2(\tau)\right), \\
\bar{R}_2 &= -\frac{1}{5}u_{1,\tau}(\tau)\theta_{1,\tau}(\tau) - \frac{13}{105}\theta_1^2(\tau)u_{1,\tau}(\tau)\theta_{1,\tau}(\tau) - \frac{9}{7}u_{2,\tau}(\tau)\theta_{1,\tau}(\tau) \\
&\quad - \frac{279}{385}\theta_1^2(\tau)u_{2,\tau}(\tau)\theta_{1,\tau}(\tau) - \frac{34}{91}\theta_1(\tau)\theta_2(\tau)u_{2,\tau}(\tau)\theta_{1,\tau}(\tau) - \frac{13}{35}\theta_2^2(\tau)u_{2,\tau}(\tau)\theta_{1,\tau}(\tau) \\
&\quad - \frac{13}{105}u_1(\tau)\theta_1(\tau)\theta_{1,\tau}^2(\tau) - \frac{279}{385}u_2(\tau)\theta_1(\tau)\theta_{1,\tau}^2(\tau) - \frac{1}{5\pi}\alpha\theta_2(\tau)\theta_{1,\tau}^2(\tau) \\
&\quad - \frac{17}{91}u_2(\tau)\theta_2(\tau)\theta_{1,\tau}^2(\tau) + \frac{13}{35}u_{1,\tau}(\tau)\theta_{2,\tau}(\tau) - \frac{7}{5}u_{2,\tau}(\tau)\theta_{2,\tau}(\tau) \\
&\quad - \frac{17}{91}\theta_1^2(\tau)u_{2,\tau}(\tau)\theta_{2,\tau}(\tau) - \frac{26}{35}\theta_1(\tau)\theta_2(\tau)u_{2,\tau}(\tau)\theta_{2,\tau}(\tau) - \frac{2}{5\pi}\alpha\theta_1(\tau)\theta_{1,\tau}(\tau)\theta_{2,\tau}(\tau) \\
&\quad - \frac{34}{91}u_2(\tau)\theta_1(\tau)\theta_{1,\tau}(\tau)\theta_{2,\tau}(\tau) - \frac{26}{35}u_2(\tau)\theta_2(\tau)\theta_{1,\tau}(\tau)\theta_{2,\tau}(\tau) \\
&\quad - \frac{13}{35}u_2(\tau)\theta_1(\tau)\theta_{2,\tau}^2(\tau) + \frac{27}{35\pi}\alpha\theta_2(\tau)\theta_{2,\tau}^2(\tau)
\end{aligned}$$

Also in Eqs. (4.25), the following expressions are used

$$\begin{aligned}
\Delta_1 &= \frac{2}{15}u_1(\tau) + \frac{6}{7}u_2(\tau), \\
\Gamma_1 &= \frac{7}{15}u_2(\tau) - \frac{1}{3\pi}\alpha - \frac{13}{105}u_1(\tau), \\
\Delta_2 &= \frac{4}{3\pi}\alpha + \frac{44}{105\pi}u_1(\tau) - \frac{4}{15\pi}u_2(\tau), \\
\Gamma_2 &= \frac{2}{63}u_1(\tau) + \frac{6}{55}u_2(\tau), \\
\Delta_3 &= -\frac{56}{15}\theta_1(\tau) + \frac{1712}{945}\theta_1^3(\tau) - \frac{152}{105}\theta_2(\tau), \\
\Gamma_3 &= -\frac{76}{105}\theta_1(\tau) - \frac{124}{63}\theta_2(\tau), \\
\Delta_4 &= -\frac{8}{63}\theta_1(\tau) - \frac{88}{135}\theta_2(\tau), \\
\Gamma_4 &= -\frac{44}{135}\theta_1(\tau) + \frac{92}{495}\theta_2(\tau)
\end{aligned}
\tag{4.26}$$

4.3 The Effect of Including Higher Order Mode Shapes

In previous sections I derived the approximated equations governing the vibration of an extensible elastic beam considering either the first mode shape or the first and second mode shapes in Galerkin's method. Inclusion of more mode shapes leads to more accurate solution. However, this needs working with higher order ODEs with more complicated terms. In this section I compare the numerical solution of the final ODEs obtained for Case I, $N = 1$ and Case II, $N = 2$ in Galerkin mode shape expansion, i.e. Eqs. (4.17) and (4.24) respectively. The numerical solution is obtained by using the Runge-Kutta method. The simulation is performed for the undamped free vibration of a beam with different μ and λ . The time history of maximum transversal deflection of the beam v_{max} are compared and results are shown in Figs. (4.3), (4.4), (4.6) and (4.7). In all figures the black line represents the simulation results for Case I and the grey line represents the results for Case II. Numerical

simulations show that for a fixed λ , by increasing the slenderness ratio, the difference between Case I and II decreases (See Figs. (4.3), (4.4)). Figure (4.4) shows that even for a long period of time, there is always a very good match between Case I and II for large μ . The frequency difference between Case I and II for $\lambda = 0$ and different values of μ is shown in Fig. (4.5). Also results show that for a fixed μ by increasing λ one gets similar results from both Case I and II (See Figs. (4.6), (4.7)).

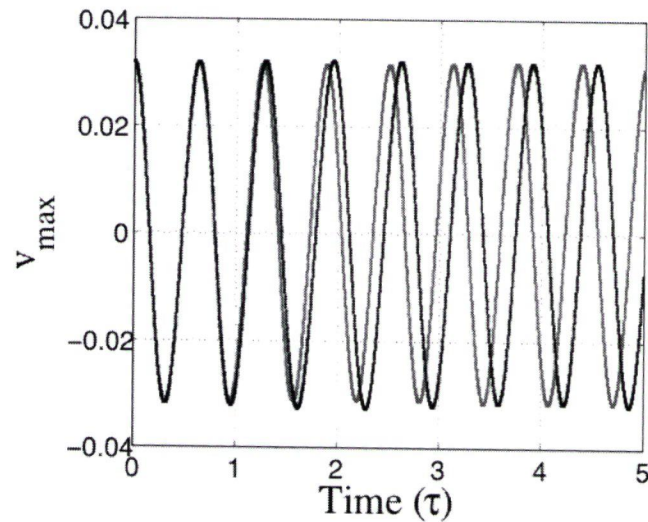


Figure 4.3: Dynamics of maximum transversal deflection of the beam in Case I and Case II, $\mu = 10$, $\lambda = 0$

Dynamic Solution, Alternative Derivations

By employing the Galerkin's method one can also approximate the PDEs of 1D extensible model, Eq.(2.70) and inextensible model, Eq. (2.81) by a second order differential equations. For both cases the transversal deflection are expressed as [28, 7]

$$v(\xi, \tau) = \sum_{n=1}^N v_n(\tau) \sin [n\pi\xi] \quad (4.27)$$

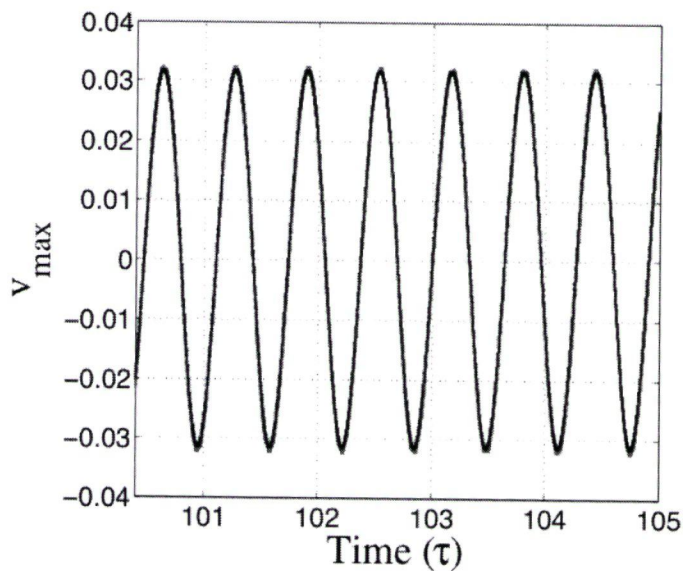


Figure 4.4: Dynamics of maximum transversal deflection of the beam in Case I and Case II, $\mu = 100$, $\lambda = 0$

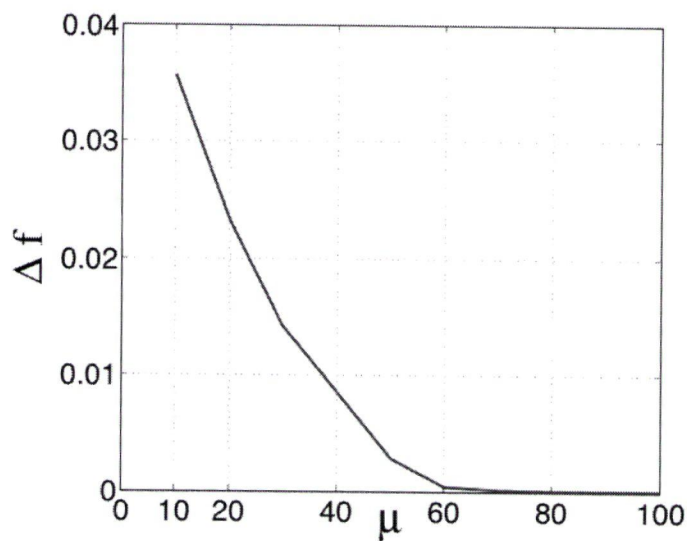


Figure 4.5: Frequency difference between Case I and Case II, $\lambda = 0$

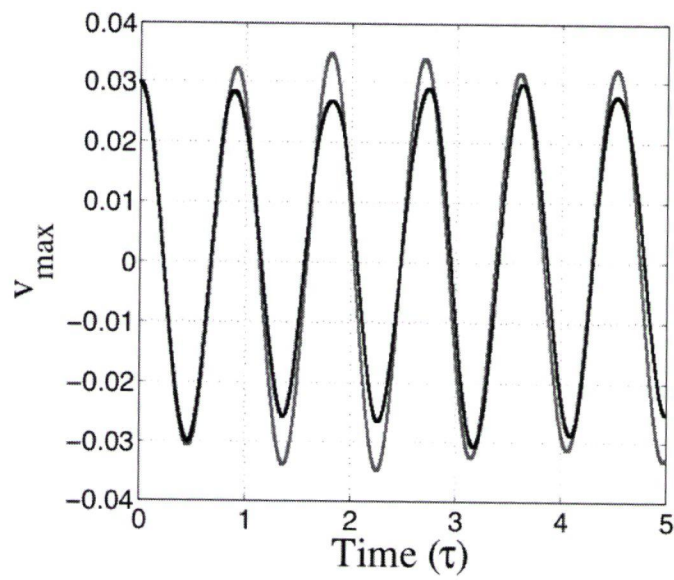


Figure 4.6: Dynamics of maximum transversal deflection of the beam in Case I and Case II, $\mu = 10$, $\lambda = 5$

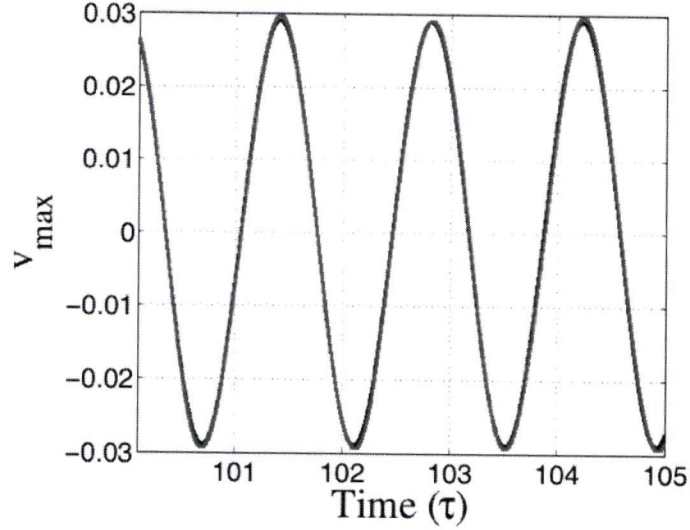


Figure 4.7: Dynamics of maximum transversal deflection of the beam in Case I and Case II, $\mu = 10$, $\lambda = 9$

Considering the first mode shape expansion, $N = 1$, substituting the above equation into the partial differential equations governing the vibration of 1D extensible beam and integrating over the length of the beam, one obtains

$$v_{1,\tau\tau}(\tau) + Cv_{1,\tau}(\tau) + \pi^2(\lambda - \pi^2)v_1(\tau) - \frac{1}{4}\pi^4\mu^2v_1^3(\tau) + \frac{4}{\pi}f_1(\tau) = 0 \quad (4.28)$$

And from Eq. (2.81), inextensible model one gets

$$v_{1,\tau\tau}(\tau) + Cv_{1,\tau}(\tau) + \pi^2(\lambda - \pi^2)v_1(\tau) - \frac{1}{2}\pi^6\mu^2v_1^3(\tau) - \frac{3}{32}\pi^8v_1^5(\tau) + \frac{4}{\pi}f_1(\tau) = 0 \quad (4.29)$$

In the next chapters I study the free and forced vibration of different models of the beam by solving the ODEs obtained in this chapter for 2D extensible model, Eq. (4.17), 1D extensible model, Eq. (4.28) and inextensible model, Eq.(4.29).

Chapter 5

Free Vibrations

Free nonlinear vibrations of an extensible elastic beam are studied in this chapter. The effect of external axial load, which corresponds to λ , the slenderness ratio, μ , and the rotary inertia, corresponding to γ , on the natural frequency of the beam is investigated. Also the configuration of resonance curve is studied for different system parameters. The results are compared with those obtained for 1D extensible and inextensible models.

5.1 Free Vibrations of Extensible Beams

Presented results of numerical simulations of the 2D extensible beam equations are obtained by using the Rung-Kutta 7th & 8th order method (See Appendix A). In all simulations the beam is assumed to be undamped and without excitation, ($C = 0$ and $f_1(\tau) = 0$ in Eqs. (4.24)). Figure (5.1) shows the maximum axial, $u(\tau)$, and transversal, $v(\tau)$ displacement for $\lambda = 9$ and different μ . For these values the beam remains not buckled. Results show that the amplitude of vibration in the axial direction is small (about 10 % of transversal amplitude of vibration). The frequency of the axial vibration is twice as large as the frequency of vibration in the transversal direction. The vibrations in transversal direction is around the straight position of the beam and the small vibrations in the axial direction is around the constant initial axial position. As μ increases, the frequencies of vibrations in both directions decrease.

In Fig. (5.2), the influence of the parameter λ , which corresponds to the axial force, on the transversal vibration of the beam is shown. For small values of λ , the

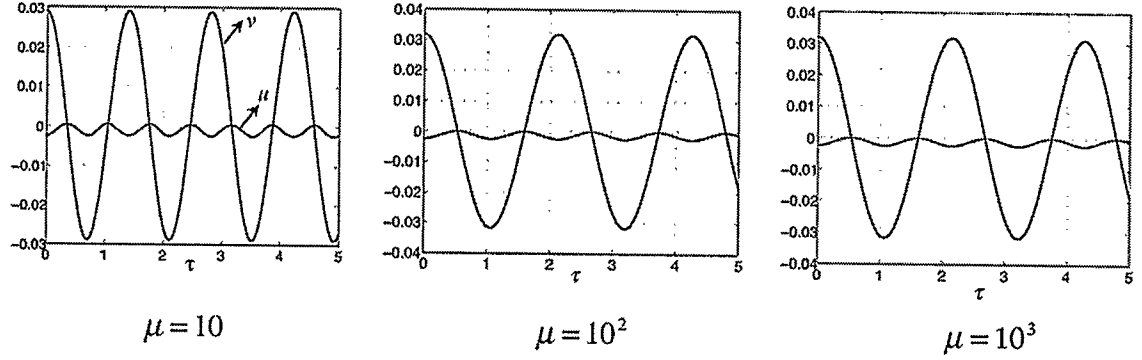


Figure 5.1: Axial and transversal displacements versus time

beam is not buckled and the vibrations in the transversal direction is around the straight beam position. When the axial force becomes equal to the buckling load, $\lambda = \lambda_{cr}$, the beam (is no longer straight) buckles. This is an equilibrium position and the frequency of vibration at this position is zero. Increasing the axial force further increases the buckling of the beam and vibrations are now centered around the buckled shape. For simulations in this part, $\mu = 10$ is used. For this value of μ the first buckling load is $\lambda_{cr} = 11.10219$ (See Eq. (3.19)).

In Fig. (5.3), the influence of λ on the natural frequency of transversal vibrations for different values of μ is depicted. Results show that, for the unbuckled beam, the larger λ results in smaller frequency of vibration. At $\lambda = \lambda_{cr}$ the natural frequency is zero and for the buckled beam the larger λ results in larger frequency of vibration. For $\mu = 10$ the buckling load is shown in the figure as $\lambda_{cr,2}$. For $\mu = 100$ $\lambda_{cr} = 9.879$ and for $\mu = 1000$ $\lambda_{cr} = 9.869$ and both are represented as $\lambda_{cr,1}$ in Fig. (5.3).

Similarly, Fig. (5.4) shows the variations of natural frequency for different models with $\mu = 1000$. As can be observed from this figure, the variations of natural frequency for different values of λ in 1D extensible and inextensible models is qualitatively

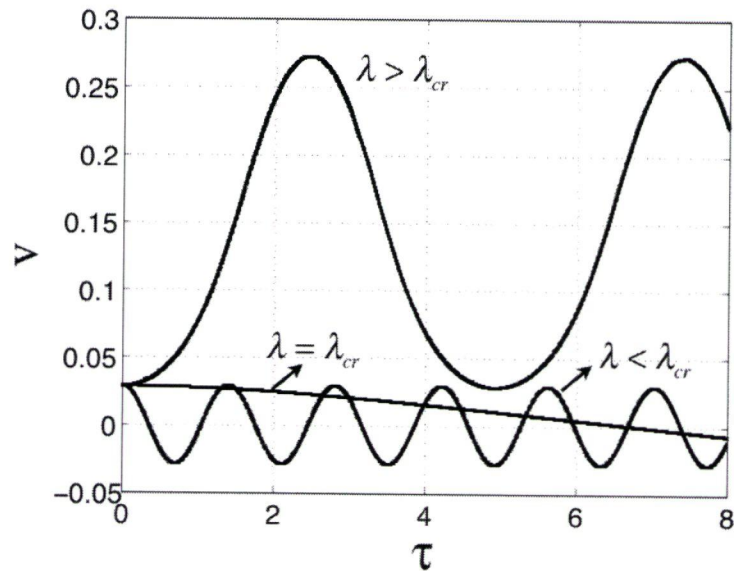


Figure 5.2: Transversal vibration for $\mu = 10$ and different values of λ

similar to the variations of natural frequency in 2D slender (large μ) extensible model

The effect of rotary inertia on the natural frequency of transversal vibrations is depicted in Fig. (5.5). Results show that for the unbuckled and buckled beam, by increasing γ , which represents the mass moment of inertia of the beam, the natural frequency decreases. Also numerical solutions show that the natural frequency of unbuckled beam is always larger than that of the buckled beam. The same trend is observed for beams with a large μ .

The natural frequency of the nonlinear vibrations depends on the initial conditions and hence the natural frequency changes as the amplitude of vibrations increases. The relationship between natural frequency and amplitude of vibration can be shown

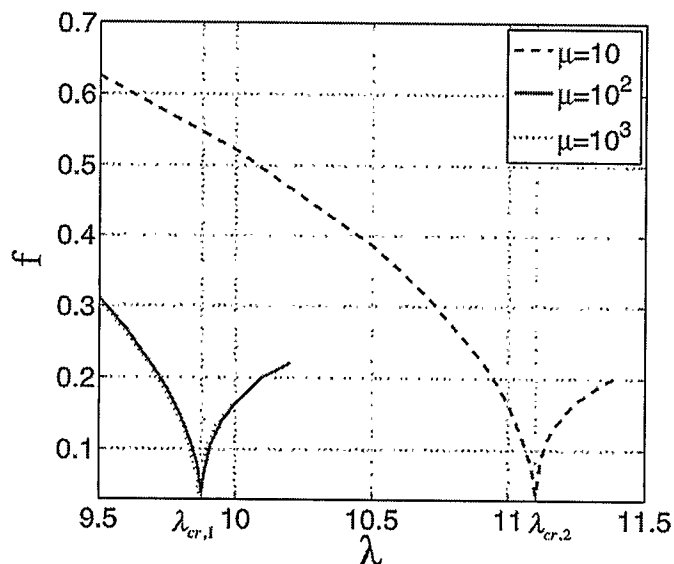


Figure 5.3: Influence of axial force, λ , on the natural frequency of transversal vibrations

with a curve named *backbone curve* [43]. The backbone curve is an important tool in the understanding the nonlinear resonance curve and defines the natural frequency as a function of the amplitude of response of the system without damping. For a linear oscillator the backbone curve is a vertical line at $\omega = \omega_n$, in the frequency-amplitude diagram, where ω_n is the natural frequency. For a nonlinear systems the backbone curve may either lean to the right (hardening nonlinearity) or to the left (softening nonlinearity). In Fig. (5.6) the resonance curve of a nonlinear system with hardening nonlinearity and also a system with softening nonlinearity and the associated backbone curves are shown. In this figure ω_1 is the natural frequency of vibration for very small amplitudes.

In Fig. (5.7) the backbone curve for different values of μ and for the unbuckled beam, $\lambda = 0$ are plotted. Results show that a short beam (small μ), exhibits softening

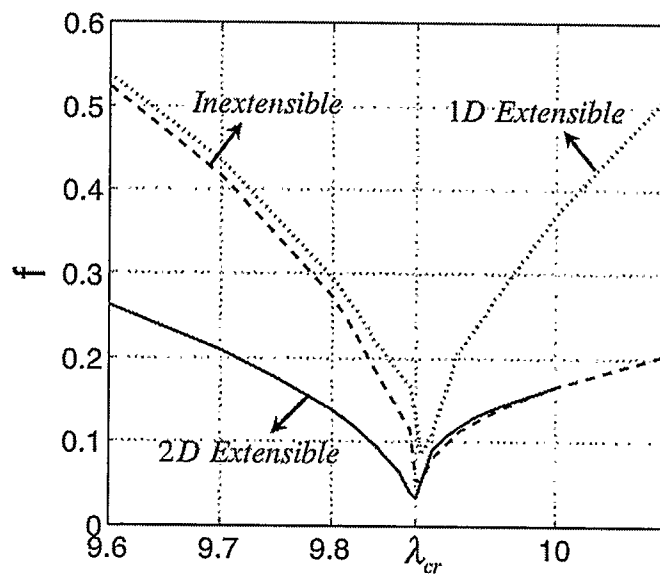


Figure 5.4: Influence of the axial force, λ , on the natural frequency of transversal vibrations in different beam models, $\mu = 1000$

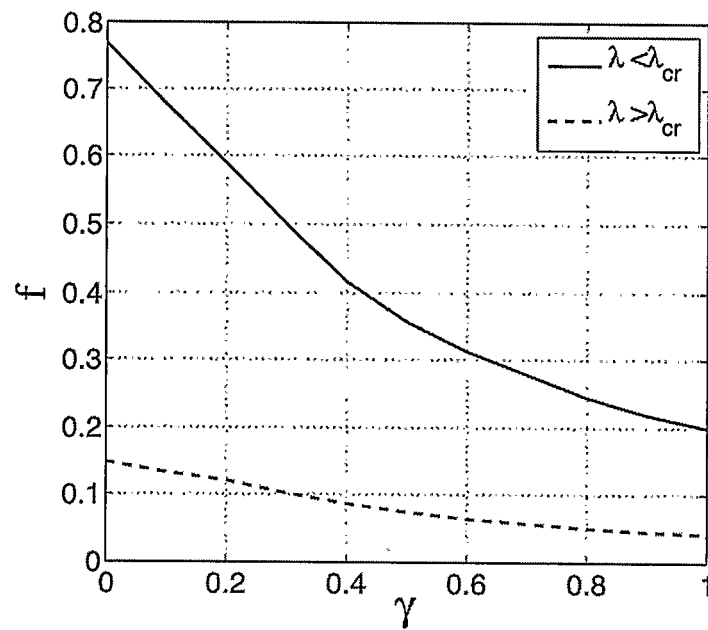


Figure 5.5: The rotary inertia effect on the natural frequency of transversal vibration, $\mu = 10$

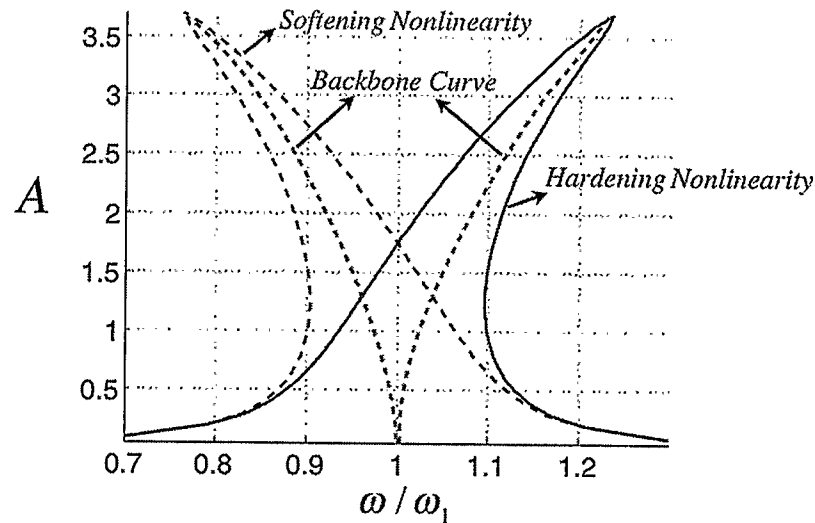


Figure 5.6: Frequency response for a nonlinear system showing (a) the backbone curve for the free undamped vibrations and (b) the resonance curve for forced damped system with hardening and softening nonlinearity

nonlinearity. For slender beams (large μ), hardening nonlinearity is observed. The softening type of nonlinearity in the simply supported beams was first recognized by Alturi [2]. He showed that the first mode of beams with one free end exhibits a softening nonlinearity and concluded that axial inertia is the dominant nonlinearity in these beams. For a short beam the axial deformation and inertia effects are more pronounced than in a slender one. Hence, according to Alturi's investigation, one expects the softening nonlinearity for the beam with small μ and the result in Fig. (5.7) verifies that. However by increasing the slenderness ratio the effect of axial inertia terms will reduce and eventually leads to a situation in which the beam exhibits hardening nonlinearity. The 1D extensible model exhibits hardening nonlinearity and the inextensible model exhibits softening nonlinearity for different slenderness ratios [40]. Numerical simulations are also performed for the buckled extensible short beam

($\mu = 10, \lambda = 11.2$) and slender beam ($\mu = 100, \lambda = 9.9$). Results show that the same trend as shown in Fig. (5.7) exists for the buckled beam, i.e. short beam exhibits softening type of nonlinearity and slender beam has hardening nonlinearity.

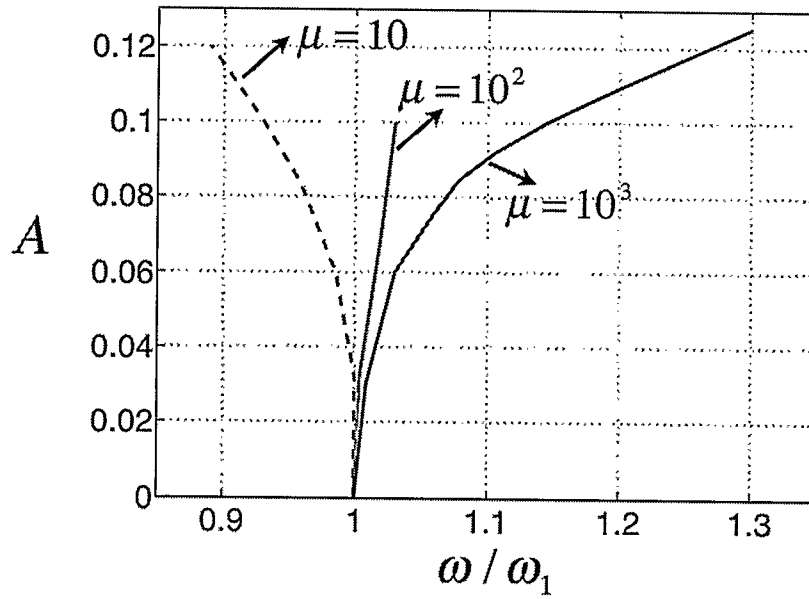


Figure 5.7: Amplitude versus natural frequency for different slenderness ratios, $\lambda = 0$

In summary, numerical results show that for the unbuckled 2D extensible beam, an increase of the axial force, λ , decreases natural frequency. At $\lambda = \lambda_{cr}$ the natural frequency is zero and for the buckled beam the larger λ results in larger frequency of vibration. The variations of natural frequency for different axial forces in 1D extensible and inextensible models are similar to variations of natural frequency in 2D slender (large μ) beams. Furthermore, for the unbuckled and buckled 2D extensible beam, an increase of the rotary inertia term, decreases the natural frequency. The rotary inertia effect is not considered in 1D extensible and inextensible models. Also results show that a short (small μ) 2D extensible unbuckled/buckled beam exhibits

softening nonlinearity while in a slender (large μ) beam hardening nonlinearity is observed. The 1D extensible model exhibits hardening nonlinearity only and the inextensible model exhibits softening nonlinearity only.

Chapter 6

Forced Vibrations and Chaos

The possibility of chaotic responses in forced vibrations of 2D extensible elastic beams is investigated in this chapter by numerical calculation of the largest Lyapunov exponent. The chaotic behavior is investigated for different amplitudes and frequencies of excitation. The results are compared with those obtained for 1D extensible and inextensible models.

6.1 Lyapunov Exponents

For investigating the forced vibrations and chaos in motion of elastic extensible beams I consider the spectrum of Lyapunov exponents, which has proven to be one of the most useful dynamical diagnostics for chaotic systems. Lyapunov exponents are the average exponential rates of divergence or convergence of nearby orbits in the phase space. Since nearby orbits correspond to nearby identical states, exponential orbital divergence means that orbits whose initial differences are very small will soon behave quite differently and predictive ability is rapidly lost. Any system containing at least one positive Lyapunov exponent is defined to be chaotic, with the magnitude of the exponent reflecting the time scale on which system dynamics become unpredictable [46].

For systems whose equations of motion are explicitly known one can calculate the Lyapunov exponents numerically. In this part I calculate the largest Lyapunov exponent (*LLE*) based on the algorithm proposed in [46]. The system with positive *LLE* is chaotic and the system with zero *LLE* exhibits regular behavior for the

defined initial conditions. For the simulations in this part the equations obtained from first mode shape expansion of 2D extensible model, Eq. (4.17), 1D extensible, Eq. (4.28), and inextensible model, Eq. (4.29), are used.

In Fig. (6.1) the dynamics of LLE for the unforced undamped 2D elastic buckled beam (Eq. (4.17)). The test parameters are as follows: $C = 0$, $f_1(\tau) = 0$, $\lambda = 11.15$, $\mu = 10$, $\gamma = 0$ and initial conditions $[0.01 \ 0 \ -0.00025 \ 0]^T$ is shown. Behavior of the beam is regular in this case and hence the LLE eventually converges to zero.

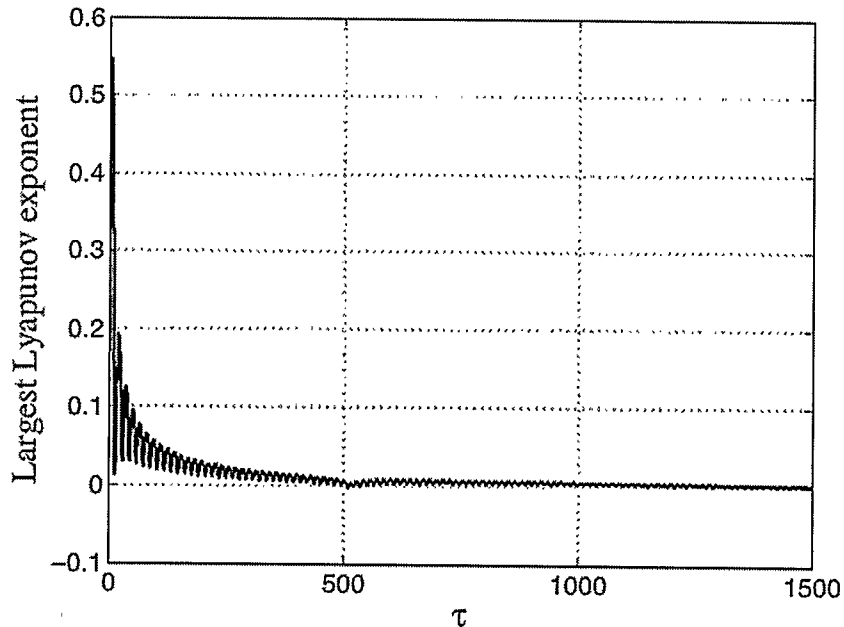


Figure 6.1: Dynamics of largest Lyapunov exponent for a beam with regular behavior

In Fig. (6.2) the dynamics of LLE for an elastic undamped extensible buckled beam ($C = 0$, $\lambda = 11.15$, $\mu = 10$, $\gamma = 0$) with chaotic behavior is depicted. The value of LLE eventually converges to a positive value ($= 0.144$) which indicates that the system is chaotic. For numerical simulation the following values are used: Amplitude

of excitation, $\mathcal{A} = 0.024$, frequency of excitation, $\Omega = 2.5$, and initial conditions, $[0.01 \ 0 \ -0.00025 \ 0]^T$.

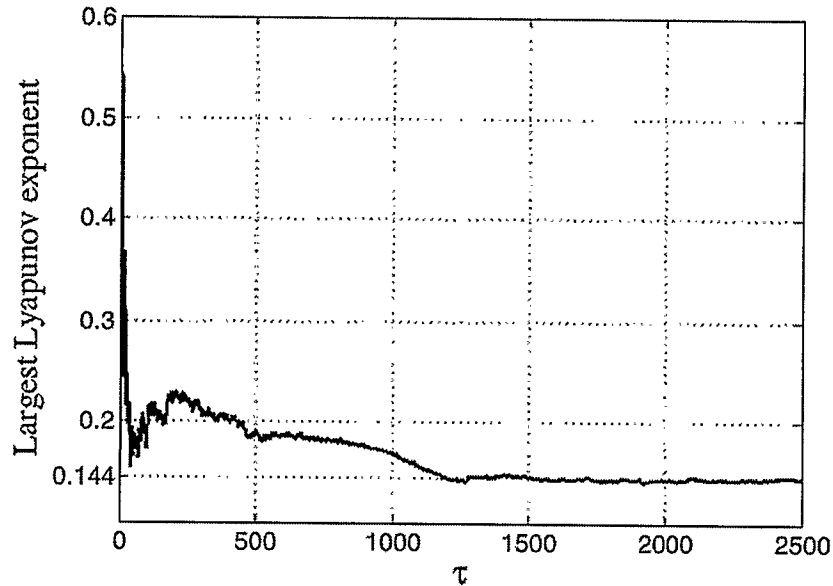


Figure 6.2: Dynamics of largest Lyapunov exponent for a beam with chaotic behavior

In Fig. (6.3) the variations of LLE for a specific buckled beam with $\mu = 10$, $\lambda = 11.15$, $\gamma = 0$, $\mathcal{A} = 0.024$ and fixed initial condition, $[0.01 \ 0 \ -0.00025 \ 0]^T$, and for different frequencies of excitations are shown. Results show that for a fixed amplitude of excitation, by increasing the frequency of excitation the LLE increases and it has the maximum value near the natural frequency of vibration. Beyond this maximum point, increasing the excitation frequency results in a reduction of LLE and for $\Omega > 5$ it is zero, i.e. the beam features regular behavior.

Figure (6.4) shows the values of LLE for a fixed excitation frequency, $\Omega = 0.05$, and different amplitudes of excitation. The system parameters are the same as those used for obtaining the results shown in Fig. (6.3). Results show that for a fixed

excitation frequency, by increasing the amplitude of excitation the LLE increases and its value eventually saturates.

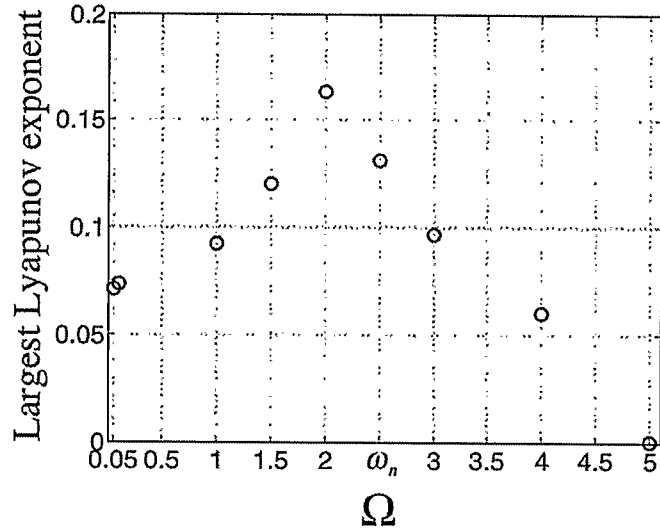


Figure 6.3: Largest Lyapunov exponent versus frequency of excitation for a 2D extensible beam

In Fig. (6.5), LLE for 1D extensible and inextensible models are shown. Here the system parameters and initial conditions, for $v(\tau)$ and $v_\tau(\tau)$, $[0.0028 \ 0]$, are the same as those used for calculating LLE for 2D extensible beam (Fig. (6.3)). Results show that for a wider range of excitation frequency, in comparison with 2D extensible model, the system behaves chaotically. For example at $\Omega = 5$ the 2D extensible model has zero LLE and hence shows regular behavior, while the other two models, 1D extensible and inextensible, have positive LLE and therefore it has chaotic motion. The time history of maximum transverse displacement for the three different beam models are shown in Fig. (6.6). Clearly, the 1D extensible and inextensible models feature chaotic pattern in time history of transverse displacement while 2D extensible

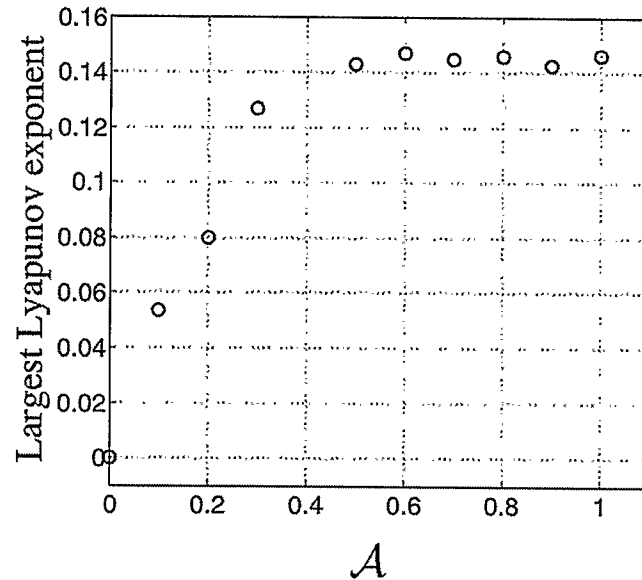


Figure 6.4: Largest Lyapunov exponent versus amplitude of excitation for a 2D extensible beam

model has regular pattern.

One can also study the chaotic behavior of 1D extensible and inextensible models by employing the *Poincaré* map. The dimension of equations for forced vibrations of 1D extensible or inextensible beam is three and hence the *Poincaré* 2D map can be shown for these models. Note that for the 2D extensible model, and for the first mode shape expansion, the dimension of the system is five and *Poincaré* map with one *Poincaré* surface is not applicable for studying chaos in this model. In Fig. (6.7) the *Poincaré* map of inextensible and 1D extensible models for $\Omega = 5$, $\mathcal{A} = 0.024$ are depicted. As shown in Fig. (6.5) the system for initial conditions $[0.0028 \ 0]$ has chaotic vibrations. The *Poincaré* maps also show that this initial condition is in the chaotic region.

Numerical results show that different models, i.e. 2D extensible, 1D extensible and

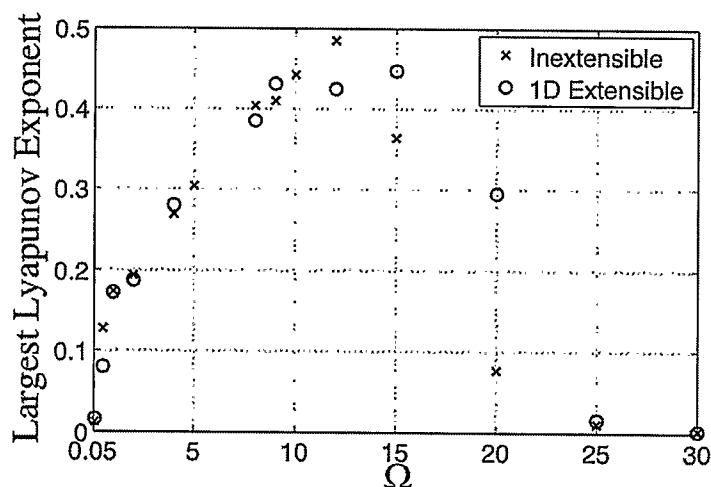


Figure 6.5: Largest Lyapunov exponent versus frequency of excitation for a 1D extensible and inextensible model

inextensible models, exhibits different forced vibrations behavior. The most accurate model, i.e. 2D extensible beam, for a short buckled beam and at a specific amplitude and frequency of vibrations ($\mathcal{A} = 0.024$ and $\Omega = 5$) has regular behavior, while the simplified models, i.e. inextensible and 1D extensible beams, exhibits chaotic behavior. The simulations are also performed for a slender buckled beam with $\mu = 400$, $\lambda = 9.9$, $C = 0$ and $\gamma = 0$. For $\mathcal{A} = 0.024$ and $\Omega = 1.5$ and the initial conditions $[0.1 \ 0 \ -0.0025 \ 0]$ (or $[0.0318 \ 0]$ for the inextensible and 1D extensible case), the 2D extensible and the inextensible models have a positive *LLE* and hence the beam motions is chaotic in both models. In contrast, the 1D extensible beam has zero *LLE* and has periodic vibrations with a high frequency. The time history of the three models for this case are compared in Fig. (6.8).

In summary, numerical results show that for a fixed amplitude of excitation and in the 2D extensible model, by increasing the frequency of excitation the largest Lyapunov

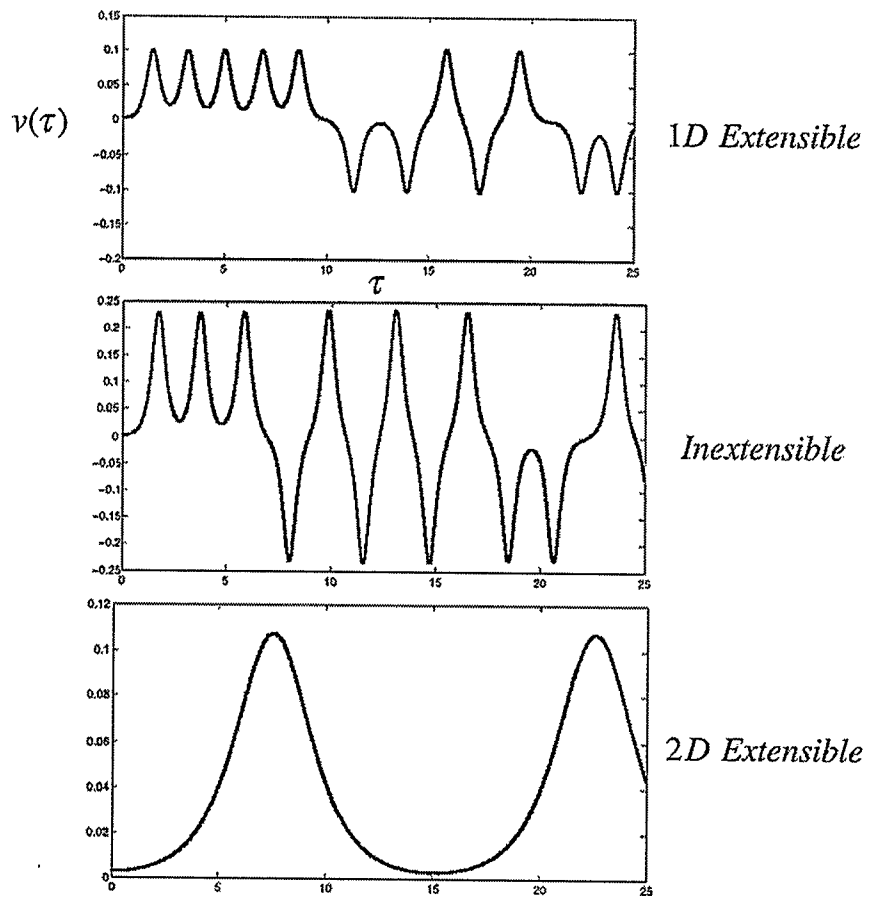


Figure 6.6: Time history of transverse displacement for different beam models, $\mu = 10$

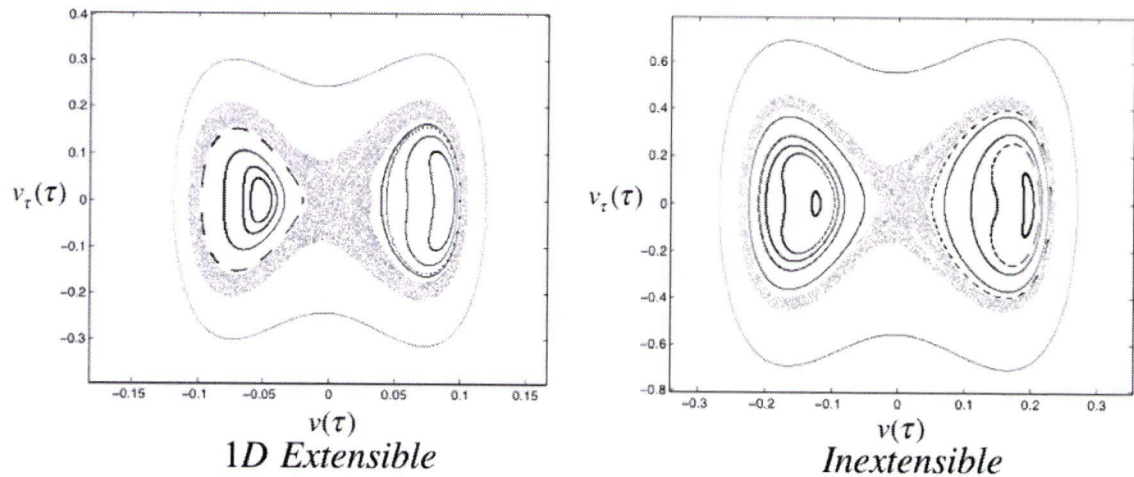


Figure 6.7: *Poincaré* map of 1D extensible and inextensible models

apunov exponent (LLE) increases and it has the maximum value near the natural frequency of vibration. Beyond this maximum point, increasing the excitation frequency results in reduction of LLE and finally it reaches zero, i.e. the system has regular behavior. Furthermore, for a fixed excitation frequency and in the 2D extensible model, by increasing the amplitude of excitation the LLE increases and its value eventually saturates. Also for a fixed amplitude of excitation, the 1D extensible and inextensible models have chaotic behavior in a wider range of excitation frequency (in comparison with 2D extensible model). Results show that different models, i.e. 2D extensible, 1D extensible and inextensible models, exhibits quite different forced vibrations behavior. The most accurate model, i.e. 2D extensible model has regular behavior for a small value of μ and at a specific amplitude and frequency of vibration, while the simplified models, i.e. inextensible and 1D extensible, exhibits chaotic behavior. In another case the 2D extensible and the inextensible models have chaotic vibration while the 1D extensible beam has periodic vibration.

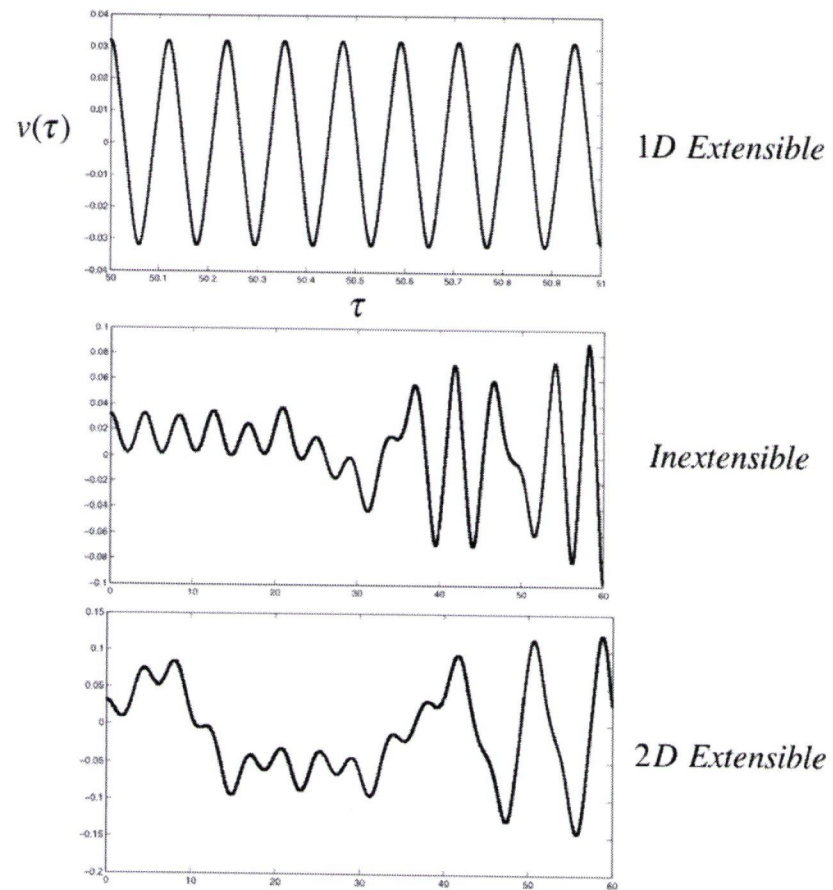


Figure 6.8: Time history of transverse displacement for different beam models, $\mu = 400$

Chapter 7

Conclusions and Future Work

In this thesis the equations governing large amplitude in-plane forced vibrations of a 2D extensible Euler-Bernoulli beam under transverse excitation are analyzed. Employing Galerkin mode shape expansion method and expanding the non-linear terms into Taylor series, these non-linear partial differential equations (PDEs) of motion are approximated by a set of coupled ordinary differential equations (ODEs). The static behavior, free (nonlinear) vibration and chaotic vibration of 2D extensible beam are analyzed and the results are compared with those obtained from previous simplified derivations, i.e. 1D extensible and inextensible models. The main conclusions of this research are as follows.

Static analysis:

- (i) An increase in slenderness ratio, μ , or in axial load, λ , increases the difference between the results of 2D extensible model with the results of 1D extensible and inextensible models.
- (ii) Higher order Taylor series expansions of the nonlinear terms lead to a more accurate postbuckling path than lower order approximations in 2D extensible model. The influence of 6th order terms and higher on postbuckling equilibrium points is limited. Therefore, in this research, 5th approximation has been used.
- (iii) The error between using exact nonlinear terms and approximated (Taylor series) nonlinear terms decreases for larger values of slenderness ratio, μ or smaller axial load, λ .

Dynamic analysis:

- (i) The partial differential equations governing vibration of 2D extensible beams are approximated using (I) first mode shape expansion and (II) first and second mode shape expansions. Results show that the single mode expansion (Case I) usually used in Galerkin methods may lead to incorrect conclusions under some conditions, especially for a beam with small λ and μ . Therefore, the second and higher order mode shapes should be included in Galerkin method.
- (ii) For the unbuckled 2D extensible beam, an increase of the axial force, λ , decreases natural frequency. At $\lambda = \lambda_{cr}$ the natural frequency is zero and for the buckled beam the larger λ results in larger frequency of vibration. The variations of natural frequency for different axial forces in 1D extensible and inextensible models are similar to variations of natural frequency in 2D slender (large μ) beams.
- (iii) For the unbuckled and buckled 2D extensible beam, an increase of the rotary inertia term, decreases the natural frequency. The rotary inertia effect is not considered in 1D extensible and inextensible models.
- (iv) For a fixed amplitude of excitation and in the 2D extensible model, by increasing the frequency of excitation the largest Lyapunov exponent (LLE) increases and it has the maximum value near the natural frequency of vibration. Beyond this maximum point, increasing the excitation frequency results in reduction of LLE and finally it reaches zero, i.e. the system has regular behavior.
- (v) For a fixed excitation frequency and in the 2D extensible model, by increasing the amplitude of excitation the LLE increases and its value eventually saturates.
- (vi) For a fixed amplitude of excitation, the 1D extensible and inextensible models have chaotic behavior in a wider range of excitation frequency (in comparison with 2D extensible model).
- (vii) Different models, i.e. 2D extensible, 1D extensible and inextensible models, ex-

hibits quite different forced vibrations behavior. The most accurate model, i.e. 2D extensible model has regular behavior for a small value of μ and at a specific amplitude and frequency of vibration, while the simplified models, i.e. inextensible and 1D extensible, exhibits chaotic behavior. In another case the 2D extensible and the inextensible models have chaotic vibration while the 1D extensible beam has periodic vibration.

This research is concerned only with mathematical models. Future works can be performed on experiments to validate the numerical results obtained in this thesis. Different beams with different slenderness ratios are needed to validate the results, for example three beams with $\mu = 10$, $\mu = 100$ and $\mu = 1000$ can be used. The experimental set-up could consist of a uniform beam supported by hinges made of radial bearings. One of the bearings should be rigidly clamped to the base and the other one should be mounted on top of a linear bearing, which permits one end of the beam to move in axial direction. The external force should be applied at this end. This set-up can be mounted at the beam ends to linear bearings permitting transverse base excitations. The transverse sinusoidal excitation could be controlled by an electromagnetic shaker. Laser sensors are needed to measure the axial and transverse displacements of the beam and also the base excitation.

Appendix A

Runge-Kutta 7th and 8th order

Let an initial value problem be specified as a set of first-order differential equations

$$\dot{\mathbf{y}} = \mathbf{f}(\mathbf{y}, t), \quad \mathbf{y}(t_0) = \mathbf{y}_0 \quad (\text{A.1})$$

Where \mathbf{y} represents a vector. The Runge-Kutta 7th and 8th order method for this problem is given by the following equations

$$\mathbf{y}_{n+1} = \mathbf{y}_n + h(k_1\mathbf{c}_1 + k_6\mathbf{c}_6 + k_7\mathbf{c}_7 + k_8\mathbf{c}_8 + k_9\mathbf{c}_9 + k_{10}\mathbf{c}_{10} + k_{11}\mathbf{c}_{11}) \quad (\text{A.2})$$

where

$$k_1 = \mathbf{f}(\mathbf{y}_n, t_n),$$

$$k_2 = \mathbf{f}(\mathbf{y}_n + k_1h_4, t_n + h_4),$$

$$k_3 = \mathbf{f}(\mathbf{y}_n + (k_1b_{31} + k_2b_{32})h, t_n + a_3h),$$

$$k_4 = \mathbf{f}(\mathbf{y}_n + (k_1b_{41} + k_3b_{43})h, t_n + a_4h),$$

$$k_5 = \mathbf{f}(\mathbf{y}_n + (k_1b_{51} + k_3b_{53} + k_4b_{54})h, t_n + a_5h),$$

$$k_6 = \mathbf{f}(\mathbf{y}_n + (k_1b_{61} + k_4b_{64} + k_5b_{65})h, t_n + a_6h),$$

$$k_7 = \mathbf{f}(\mathbf{y}_n + (k_1b_{71} + k_4b_{74} + k_5b_{75} + k_6b_{76})h, t_n + a_7h),$$

$$k_8 = \mathbf{f}(\mathbf{y}_n + (k_1b_{81} + k_5b_{85} + k_6b_{86} + k_7b_{87})h, t_n + a_8h),$$

$$k_9 = \mathbf{f}(\mathbf{y}_n + (k_1b_{91} + k_4b_{94} + k_5b_{95} + k_6b_{96} + k_7b_{97} + k_8b_{98})h, t_n + a_9h),$$

$$k_{10} = \mathbf{f}(\mathbf{y}_n + (k_1b_{10-1} + k_4b_{10-4} + k_5b_{10-5} + k_6b_{10-6} + k_7b_{10-7} + k_8b_{10-8} + k_9b_{10-9})h, t_n + a_{10}h),$$

$$k_{11} = f(y_n + (k_1 b_{11-1} + k_4 b_{11-4} + k_5 b_{11-5} + k_6 b_{11-6} + k_7 b_{11-7} + k_8 b_{11-8} + k_9 b_{11-9} + k_{10} b_{11-10})h), t_n + h),$$

$$k_{12} = f(y_n + (k_1 b_{12-1} + k_4 b_{12-4} + k_5 b_{12-5} + k_6 b_{12-6} + k_7 b_{12-7} + k_8 b_{12-8} + k_9 b_{12-9} + k_{10} b_{12-10})h), t_n + a_{12}h),$$

$$k_{13} = f(y_n + (k_1 b_{13-1} + k_4 b_{13-4} + k_5 b_{13-5} + k_6 b_{13-6} + k_7 b_{13-7} + k_8 b_{13-8} + k_9 b_{13-9} + k_{10} b_{13-10}) + k_{12} b_{13-12})h, t_n + h),$$

and

$$\begin{aligned} c_1 &= \frac{13}{288}, & c_6 &= \frac{32}{125}, & c_8 &= \frac{2401}{12375}, \\ c_9 &= \frac{1701}{14080}, & c_{10} &= \frac{2401}{19200}, & c_{11} &= \frac{19}{450}, \end{aligned}$$

$$\begin{aligned} a_2 &= \frac{1}{4}, & a_3 &= \frac{1}{12}, & a_4 &= \frac{1}{8}, \\ a_5 &= \frac{2}{5}, & a_6 &= \frac{1}{2}, & a_7 &= \frac{6}{7}, \\ a_8 &= \frac{1}{7}, & a_9 &= \frac{2}{3}, & a_{10} &= \frac{2}{7}, & a_{12} &= \frac{1}{3}, \end{aligned}$$

$$\begin{array}{llll}
b_{31} = \frac{5}{72}, & b_{32} = \frac{1}{72}, & b_{41} = \frac{1}{32}, & b_{43} = \frac{3}{32}, \\
b_{51} = \frac{106}{125}, & b_{53} = \frac{-408}{125}, & b_{54} = \frac{352}{125}, & b_{61} = \frac{1}{48}, \\
b_{64} = \frac{8}{33}, & b_{65} = \frac{125}{528}, & b_{71} = \frac{-13893}{26411}, & b_{74} = \frac{39936}{26411}, \\
b_{75} = \frac{-64125}{26411}, & b_{76} = \frac{60720}{26411}, & b_{81} = \frac{37}{392}, & b_{85} = \frac{1625}{9408}, \\
b_{86} = \frac{-2}{15}, & b_{87} = \frac{61}{6720}, & b_{91} = \frac{17176}{25515}, & b_{94} = \frac{-47104}{25515}, \\
b_{95} = \frac{1325}{504}, & b_{96} = \frac{-41792}{25515}, & b_{97} = \frac{20237}{145800}, & b_{98} = \frac{4312}{6075}, \\
b_{10-1} = \frac{-23834}{180075}, & b_{10-4} = \frac{-77824}{1980825}, & b_{10-5} = \frac{-636635}{633864}, & b_{10-6} = \frac{254048}{300125}, \\
b_{10-7} = \frac{-183}{7000}, & b_{10-8} = \frac{8}{11}, & b_{10-9} = \frac{-324}{3773}, & b_{11-1} = \frac{12733}{7600}, \\
b_{11-4} = \frac{-20032}{5225}, & b_{11-5} = \frac{456485}{80256}, & b_{11-6} = \frac{-42599}{7125}, & b_{11-7} = \frac{339227}{912000}, \\
b_{11-8} = \frac{-1029}{4180}, & b_{11-9} = \frac{1701}{1408}, & b_{11-10} = \frac{5145}{2432}, & b_{12-1} = \frac{-27061}{204120}, \\
b_{12-4} = \frac{40448}{280665}, & b_{12-5} = \frac{-1353775}{1197504}, & b_{12-6} = \frac{17662}{25515}, & b_{12-7} = \frac{-71687}{1166400}, \\
b_{12-8} = \frac{98}{225}, & b_{12-9} = \frac{1}{16}, & b_{12-10} = \frac{3773}{11664}, & b_{13-1} = \frac{11203}{8680}, \\
b_{13-4} = \frac{-38144}{11935}, & b_{13-5} = \frac{2354425}{458304}, & b_{13-6} = \frac{-84046}{16275}, & b_{13-7} = \frac{673309}{1636800}, \\
b_{13-8} = \frac{4704}{8525}, & b_{13-9} = \frac{9477}{10912}, & b_{13-10} = \frac{-1029}{992}, & b_{13-12} = \frac{729}{341},
\end{array}$$

and

$$h_4 = a_2 h.$$

In the above equations h is the step size and the error in each step will be:

$$error = e_1 k_1 + e_6 k_6 + e_7 k_7 + e_8 k_8 + e_9 k_9 + e_{10} k_{10} + e_{11} k_{11} + e_{12} k_{12} + e_{13} k_{13} \quad (\text{A.3})$$

where

$$\begin{aligned} e_1 &= \frac{-6600}{3168000}, & e_6 &= \frac{-135168}{3168000}, & e_7 &= \frac{-14406}{3168000}, & e_8 &= \frac{57624}{3168000}, \\ e_9 &= \frac{54675}{3168000}, & e_{10} &= \frac{-396165}{3168000}, & e_{11} &= \frac{-133760}{3168000}, & e_{12} &= \frac{437400}{3168000}, \\ e_{13} &= \frac{136400}{3168000}. \end{aligned}$$

Bibliography

- [1] Robert A. Adams and Christopher Essex. *Calculus: A complete course*. Pearson Canada, 7th edition, 2009.
- [2] S. Alturi. Nonlinear vibrations of a hinged beam including nonlinear inertia effects. *Journal of Applied Mechanics*, 40:121–126, 1973.
- [3] S. P. Beeby, M. J. Tudor, and N. M. White. Energy harvesting vibration source for microsystems applications. *Measurement Science and Technology*, 17:175–195, 2006.
- [4] D. Burgreen. Free vibration of a pin-ended column with constant distance between pin ends. *Journal of Applied Mechanics*, 18:135–139, 1951.
- [5] L. Cveticanin and T. Atanackovic. Non-linear vibration of an extensible elastic beam. *Journal of Sound and Vibration*, 177(2):159–171, 1994.
- [6] J. G. Easley. Large amplitude vibration of buckled beams and rectangular plates. *AIAA Journal*, 2:2207–2209, 1964.
- [7] Samir A. Emam. *A theoretical and experimental study of nonlinear dynamics of buckled beams*. PhD thesis, Virginia Polytechnic Institute and State University, 2002.
- [8] Samir A. Emam and Ali H. Nayfeh. On the nonlinear dynamics of a buckled beam subjected to a primary-resonance excitation. *Nonlinear Dynamics*, 35:1–17, 2004.
- [9] A. R. Forsyth. *Calculus of variations*. Dover publications, 1960.

- [10] Herbert Goldstein, Charles Poole, and John Safko. *Classical mechanics*. Addison Wesley, 3rd edition, 2002.
- [11] S. M. Han, H. Benaroya, and T. Wei. Dynamics of transversely vibrating beams using four engineering theories. *Journal of Sound and Vibration*, 225(5):935–988, 1999.
- [12] P. J. Holmes. A nonlinear oscillator with a strange attractor. *Philosophical Transactions of Royal Society of London*, 292:419–448, 1979.
- [13] P. J. Holmes and F. C. Moon. Strange attractor and chaos in nonlinear mechanics. *Journal of Applied Mechanics*, 50:1021–1032, 1983.
- [14] W. Lacarbonara and H. Yabuno. Refined models of elastic beams undergoing large in-plane motions: Theory and experiment. *International Journal of Solids and Structures*, 43:5066–5084, 2006.
- [15] W. Lestari and S. Hanagud. Nonlinear vibrations of buckled beams: Some exact solutions. *International Journal of Nonlinear Mechanics*, 38:4741–57, 2001.
- [16] A. Magnusson, M. Ristinmaa, and C. Ljung. Behaviour of the extensible elastica solution. *International Journal of Solids and Structures*, 38:8441–8457, 2001.
- [17] B. P. Mann and B. A. Owens. Investigations of a nonlinear energy harvester with a bistable potential well. *Journal of Sound and Vibration*, 329:1215–1226, 2010.
- [18] Corrado Maurini, Joël Pouget, and Stefano Vidoli. Distributed piezoelectric actuation of a bistable buckled beam. *European Journal of Mechanics A/Solids*, 26:837–853, 2007.

- [19] P. H. McDonald. Nonlinear dynamic coupling in a beam vibration. *Journal of Applied Mechanics*, 22:573–578, 1955.
- [20] C. R. McInnes, D. G. Gorman, and M. P. Cartmell. Enhanced vibration energy harvesting using nonlinear stochastic resonance. *Journal of Sound and Vibration*, 318:655–662, 2008.
- [21] C. Mei and K. Decha-Umphai. A finite element method for non-linear forced vibrations of beams. *Journal of Sound and Vibration*, 102(3):369–380, 1985.
- [22] Loenard Meirovitch. *Fundamentals of vibration*. McGraw-Hill, 2001.
- [23] J. Meohlis, B. E. DeMartini, J. L. Rogers, and K. L. Turner. Exploiting nonlinearity to provide broadband energy harvesting. Proceedings of the ASME 2009 Dynamic Systems and Control Conference, 2009.
- [24] G. B. Min and J. G. Easley. Nonlinear vibrations of buckled beams. *Journal of Engineering for Industry*, 94:637–646, 1972.
- [25] F. C. Moon. Experiments on chaotic motions of a forced nonlinear oscillator: Strange attractor. *Journal of Applied Mechanics*, 47:638–648, 1980.
- [26] Francis C. Moon. *Chaotic vibrations*. Wiley Interscience, 2004.
- [27] Ali H. Nayfeh and Samir A. Emam. Exact solution and stability of postbuckling configurations of beams. *Nonlinear Dynamics*, 54:395–408, 2008.
- [28] S. P. M. Noijen, N. J. Mallon, and R. H. B. Fey. Periodic excitation of a buckled beam using a higher order semianalytic approach. *Nonlinear Dynamics*, 50:325–339, 2007.

- [29] Seunghoon Park. A study on buckled beam actuators for RF MEMS applications. Master's thesis, Louisiana State University, 2005.
- [30] E. P. Popov, S. Nagarajan, and Z. A. Lu. *Mechanics of materials*. Prentice Hall, 2nd edition, 1978.
- [31] Jin Qiu, Jeffrey H. Lang, and Alexander H. Slocum. A curved-beam bistable mechanism. *Journal of Microelectromechanical Systems*, 13(2):137–146, 2004.
- [32] E. Quevy, P. Biggote, D. Collard, and L. Buchaillot. Large stroke actuation of continuous membrane for adaptive optics by 3D self-assembled microplates. *Sensors Actuators*, A95:183–195, 2002.
- [33] R. Ramlan, M. J. Brennan, B. R. Mace, and I. Kovacic. Potential benefits of a nonlinear stiffness in an energy harvesting device. *Nonlinear Dynamics*, 59:545–558, 2010.
- [34] Singiresu S. Rao. *Mechanical vibrations*. Addison Wesley, 1990.
- [35] T. S. Reynolds and E. H. Dowell. The role of higher modes in the chaotic motion of the buckled beam. *International Journal of Nonlinear Mechanics*, 31:931–939, 1996.
- [36] M. Taher A. Saif. On a tunable bistable mems-theory and experiments. *Journal of Microelectromechanical Systems*, 9(2):157–170, 2000.
- [37] C. Semler, G. X. Li, and M. P. Paidoussis. The non-linear equations of motion of pipes conveying fluid. *Journal of Sound and Vibration*, 1169(5):577–599, 1994.
- [38] S. V. Sorokin and A. V. Terentiev. On the optimal design of the shape of a buckled elastic beam. *Structural and Multidisciplinary Optimization*, 21:60–68,

2001.

- [39] D. M. Tang and E. H. Dowell. On the threshold force for chaotic motions for a forced buckled beam. *Journal of Applied Mechanics*, 55:190–196, 1988.
- [40] Jon J. Thomsen. *Vibrations and Stability, Advanced Theory, Analysis and Tools*. Springer, 2003.
- [41] W. Y. Tseng and J. Dugundji. Nonlinear vibrations of a buckled beam under harmonic excitation. *Journal of Applied Mechanics*, 38:467–476, 1971.
- [42] Lawrence N. Virgin. *Vibration of axially loaded structures*. Cambridge University Press, 2007.
- [43] David Wagg and Simon Neild. *Nonlinear Vibration with Control*. Springer, 2010.
- [44] J. Winterflood, T. Barber, and D. G. Blair. Using euler buckling springs for vibration isolation. *Classical Quantum Gravity*, 19(7):1639–1645, 2002.
- [45] S. Woinowsky-Kreiger. The effect of an axial force on the vibration of hinged bars. *Journal of Applied Mechanics*, 7:35–36, 1950.
- [46] Alan Wolf, Jack B. Swift, Harry L. Swinney, and John A. Vastano. Determining Lyapunov exponents from a time series. *Physica D*, pages 285–317, 1985.